The Thesis committee for Kelly Alaine Regimbal
Certifies that this is the approved version of the following thesis:

Improving resolution of NMO stack using shaping regularization

APPROVED BY

SUPERVISING COMMITTEE:

Sergey Fomel, Supervisor

Kyle Spikes

Chris Zahm

Improving resolution of NMO stack using shaping regularization

by

Kelly Alaine Regimbal, B.S.

THESIS

Presented to the Faculty of the Graduate School of

The University of Texas at Austin

in Partial Fulfillment

of the Requirements

for the Degree of

Master of Science in Geological Sciences

THE UNIVERSITY OF TEXAS AT AUSTIN

May 2016

Dedicated to all of my family, friends and professors who have provided support and encouragement over the years.

Acknowledgments

I am deeply grateful for the many individuals who have supported me over the years and contributed to the production of this thesis.

Foremost, I would like to thank my advisor, Dr. Sergey Fomel, for his inspiring ideas and large contributions towards this thesis. I have been very fortunate to have an advisor who gave me the freedom to explore on my own, but at the same time, provided guidance when needed. Coming from a mathematical background, I have learned a great deal about the field of geophysics from his guidance, patience, and immense knowledge. My most sincere thanks goes to Sergey for introducing me to the curiosities and challenges of scientific research.

I would like to thank the rest of my thesis committee: Dr. Chris Zahm and Dr. Kyle Spikes, for their insightful feedback and improvements to this thesis. My thanks goes to Philip Guerrero for making my experience at the University of Texas at Austin a memorable one.

The members of the Texas Consortium of Computational Seismology (TCCS) have been nothing less than enlightening and inspirational during my time at the University of Texas at Austin. I have been fortunate to be surrounded by hard-working individuals that have been a tremendous support in terms of technical help and encouraging discussions. I am also thankful for the financial support from sponsors of the TCCS.

Numerical experiments and processing for this thesis were achieved using

Madagascar, which is an open-source software package for reproducible research. I am grateful to all of the Madagascar contributors who provided the tools necessary to complete the work in this thesis.

I would like to thank the many professors and mentors who have encouraged me throughout my undergraduate years at Colorado Mesa University. My thanks goes to Dr. Dan Schultz-Ela for spending numerous hours teaching me the fundamentals of geophysics and guiding me towards applying for a graduate degree. I would like to thank Dr. Ed Bonan-Hamada for inspiring me in the field of mathematics and for the constant support during my years at CMU.

Most importantly, none of this would have been possible without my loving parents, Dan and Lucy Regimbal. They receive my deepest gratitude and love for their constant encouragement and support throughout the years. Last, but not least, I am grateful for my siblings, Matt, Dylan, and Danielle, for their support, love, and comic relief over the years.

Improving resolution of NMO stack using shaping regularization

Kelly Alaine Regimbal, M.S.Geo.Sci.

The University of Texas at Austin, 2016

Supervisor: Sergey Fomel

Common midpoint (CMP) stacking is one of the major steps in seismic data processing. Traditional CMP stacking sums a combination of normal moveout (NMO) corrected traces across a CMP gather to produce a single trace with a higher signal-to-noise (S/N) ratio than that of individual traces within the gather. Several problems arise with the assumptions and principles of conventional NMO and stack. NMO correction causes undesirable distortions of signals on a seismic trace known as "NMO stretch", which lowers the frequency content of the corrected reflection event at far offsets. This violates the assumption of a uniform distribution of phase and frequency of seismic reflections across the corrected gather. Common procedures to eliminate this stretching effect involve muting all of the samples with severe distortions. This causes a decrease in fold and can destroy useful far-offset information essential for amplitude variation with offset (AVO) analysis. Inaccuracy in stretch muting with residual "stretching" effects produces a lower amplitude and lower resolution stack. I

present two methods that eliminate the effects of "NMO stretch" and restore a wider frequency band by replacing conventional NMO and stack with a regularized inversion to zero offset. The resulting stack is a model that best fits the data using additional constraints imposed by the method of shaping regularization. Shaping regularization implies a mapping of the input model to a space of acceptable models. The shaping operator is integrated in an iterative inversion algorithm and provides an explicit control on the estimated stack. I use shaping regularization to achieve a stack that has a denser time sampling and contains higher frequencies than the conventional stack. In the first approach, I define the backward operator of shaping regularization using the principles of conventional NMO correction and stack. In the second approach, I introduce a recursive stacking scheme using plane-wave construction in the backward operator of shaping regularization. The advantage of using recursive stacking along local slopes in the application to NMO and stack is that it avoids "stretching" effects caused by NMO correction and is insensitive to non-hyperbolic moveout in the data. Numerical tests demonstrate each algorithm's ability to attain a higher frequency stack with a denser temporal sampling interval compared to those of the conventional stack and to minimize stretching effects caused by NMO correction. I apply both methods to two 2-D marine datasets from the North Sea and achieve noticeable resolution improvements in the stacked sections compared with that of conventional NMO and stack. By treating NMO and stack as an iterative inversion using shaping regularization, resolution is enhanced by utilizing signal from different offsets and minimizing stretching effects to reconstruct a high resolution stack.

Table of Contents

List of Figures

Chapter 1

Introduction

In seismic data processing, common midpoint (CMP) stacking is one of the most fundamental processes (Yilmaz, 2001). Stacking combines normal moveout (NMO) corrected traces across a CMP gather to produce a single trace with a higher signal-to-noise ratio than that of individual traces within the gather (Rashed, 2014). Stacking is a simple process that has powerful properties, such as noise attenuation. Major seismic data processing steps, such as velocity analysis and migration, follow the key principles involved in the stacking concept. For these reasons, stacking is a powerful tool that continues to be a cornerstone for seismic data processing in seismic exploration.

In seismic exploration, future challenges could involve collecting more data in order to discover new unconventional resources (Rashed, 2014). Furthermore, there is a constant demand for higher resolution and better quality images of the subsurface, where more information needs to be extracted from the data. The development of alternative processing routines and efficient stacking algorithms that maintain data characteristics is the key to successfully pushing the resolution limits of the data. With increasing computational power, treating the process of stacking as an inverse problem may achieve higher quality stacked sections that contain more useful information of the subsurface. My research focuses on improving resolution of stacked sections

by recovering more information from different offsets using a regularized inversion scheme.

In this thesis, I present two alternative approaches to NMO and stack using inversion by shaping regularization. Shaping regularization involves mapping the input model to a space of acceptable models (Fomel, 2007). The shaping operator is integrated in an iterative inversion algorithm and provides an explicit control on the estimation result. I experiment with two different formulations of shaping regularization in the application of NMO and stack, which I refer to as shaping NMO stack and plane-wave construction (PWC) stack. Both approaches aim to optimize CMP stacking and enhance resolution of the final stacked seismic section by extracting more information from different offsets. Unlike conventional stacking, the spectra of the resulting high-resolution stacks are not limited by the Nyquist frequency of the input gathers.

THESIS OUTLINE

In chapter 2, I review conventional NMO and stack and flaws that arise with the assumptions and principles that set the foundation for this approach. I examine previously proposed methods that aim to improve conventional NMO and stack by eliminating "NMO stretch" and improving resolution of stacked sections. Next, I introduce "beyond Nyquist" approaches that demonstrate that stacking has the capability of utilizing more information from different offsets and is not necessarily limited by the Nyquist frequency of the input CMP gather. Finally, I review shaping regularization, which is a regularized inversion scheme that is the fundamental tool for the two stacking approaches I introduce in later chapters.

In chapter 3, I define the first method to optimize NMO and stack, which is referred to as shaping NMO stack. I conduct synthetic experiments to test the ability of this algorithm to eliminate "NMO stretch" and achieve a broader bandwidth in comparison to conventional NMO and stack.

In chapter 4, I define the second approach to improve the process of NMO and stack, which I present as plane-wave construction (PWC) stacking using shaping regularization. I test this algorithm's ability on numerical examples to demonstrate resolution improvements and the reduction of "NMO stretch".

In chapter 5, I apply both stacking methods to a 2-D field data set from the North Sea and the 2-D Viking Graben data set to evaluate the differences in each algorithm's ability to recover a broader bandwidth. I then compare the resulting stacked sections to conventional NMO and stack to demonstrate noticeable resolution improvements.

In chapter 6, I conclude this thesis with a brief discussion of the results by identifying advantages and disadvantages of the two stacking methods introduced and identifying future applications of the work presented in this thesis.

Chapter 2

Review

In this chapter, I discuss key concepts and limitations of conventional normal-moveout and stack and review previously proposed methods that aim to improve this process to reconstruct higher resolution stacked sections. I also review the basic principles of high-frequency signal recovery that set the foundation for the two stacking schemes introduced in the next chapters.

NORMAL MOVEOUT CORRECTION AND STACK

In seismic data processing, common midpoint (CMP) stacking is one of the most fundamental processes (Yilmaz, 2001). CMP stacking combines normal moveout (NMO)-corrected traces across a CMP gather to produce a single trace with a higher signal-to-noise ratio (Rashed, 2014). Many problems arise with the assumptions and principles that set the foundation for conventional NMO and stack. Conventional NMO correction transforms traces at non-zero offset into traces that are effectively at zero offset (Barnes, 1992). The travel-time $t(x)$ at offset x is related to the zero-offset travel time t_0 using the normal moveout equation:

$$t(x) = \sqrt{t_0^2 + \frac{x^2}{v(t_0)^2}}, \tag{2.1}$$

where $v(t_0)$ is the root-mean-square velocity. NMO correction is, therefore, a time coordinate transformation, where time-variant nonlinear distortions of the seismic

traces are introduced in the corrected traces (Barnes, 1992). These undesirable distortions of signals on a seismic trace are known as "NMO stretch" and result in lower frequency content of the corrected reflection event at far offsets (Dunkin and Levin, 1973), as illustrated in Figure 2.1. This violates the assumption of a uniform distribution of phase and frequency of seismic reflections across the corrected gather. Common procedures to eliminate this stretching effect involve muting samples with severe distortions. This causes a decrease in fold and can destroy useful far-offset information essential for amplitude variation with offset (AVO) analysis (Swan, 1988). Inaccuracy in stretch muting with residual "stretching" effects can also produce a lower-amplitude and lower-resolution stack (Miller, 1992).

Conventional stacking is a simple process that combines the NMO-corrected traces by summing and normalizing. Stacking is based on the assumption that useful signal is coherent, whereas noise is random. In real seismic data, coherent noise and noise bursts are common, causing inaccuracy in the conventional stack (Rashed, 2014). Traditional stacking also assumes that the NMO-corrected gather has perfectly aligned seismic reflections (Yilmaz, 2001). However, NMO correction is an approximation that assumes the travel-time as a function of offset follows a hyperbolic trajectory in a CMP gather, which might fail in common geologic settings that involve lateral velocity variations or anisotropy (Yilmaz, 2001).

Non-stretch NMO methods

Several algorithms were developed to improve CMP stacking and enhance resolution of stacked sections by reducing stretching effects. Claerbout (1992) describes inverse NMO stacking, which recasts NMO correction and stacking as an inversion process in the constant velocity case. This approach combines conventional NMO

and stack into one step by solving a set of simultaneous equations using iterative least-squares optimization. Figure 2.2 displays a reproduced synthetic experiment that illustrates Claerbout's method. The model is a zero-offset trace, and the data is a CMP gather. Iteration 0 is similar to conventional NMO and stack, which fails to recover the rectangular shaped waveform of the zero-offset trace. After just 4 conjugate gradient iterations, the zero-offset trace is accurately reconstructed. Through this simple experiment, Claerbout demonstrates that by treating NMO and stack as an inverse process, one can recover the true amplitude and spectrum of the zero-offset trace. Sun (1997) extended Claerbout's idea to the case of depth-variable velocity. The inverse NMO stack operator applied depends on the hyperbolic moveout relation and can be employed to remove non-hyperbolic events and random noise. Trickett (2003) uses a variation of Claerbout's inverse NMO stack in his stretch-free stacking method to avoid "NMO stretch". Trickett's results tend to be higher frequency but noisier than a conventional stack. Multiple other algorithms have been proposed that aim to reduce NMO-stretching effects (Byun and Nelan, 1997; Hicks, 2001; Hilterman and Schuyver, 2003; Rupert and Chun, 1975; Perroud and Tygel, 2004; Masoomzadeh et al., 2010; Zhang et al., 2013; Kazemi and Siahkoohi, 2011). Shatilo and Aminzadeh (2000) proposed a constant NMO-correction strategy, which applies a constant NMO shift within a finite-time interval that is equal to the wavelet length of a trace. This approach eliminates wavelet stretch and preserves higher frequencies than the conventional method, resulting in a higher resolution stack. However, samples that exist in overlapping time windows are used twice during the correction, resulting in an amplitude distortion. More recently, Ma et al. (2015) proposed a stacking technique based on a sparse inversion algorithm that computes the stack directly from a CMP gather by solving an optimization problem using principles of compressive sensing.

This method eliminates the stretch effect of conventional CMP stacking and improves resolution in the stacked section. Silva et al. (2015) introduced a recursive stacking approach using local slopes to compute a stack without stretching effects. This velocity-independent stacking technique starts at the farthest offset and accumulates the estimated stack until the near offset is reached.

Reconstructing a "beyond Nyquist" stack

Several stacking approaches were introduced that strive to reconstruct a higher resolution stack, where frequencies recovered are not limited by the Nyquist frequency of the input data. Wisecup (1998) introduced random sample interval imaging (RSI^2), which maps the CMP gather into the "after NMO space" using the exact moveout times and no interpolation. The NMO-corrected values are collected in the stack, rather than summed, where the input sample values are mapped to their correct time values in the stack. Stark (2013) discussed the idea of signal recovery beyond the conventional Nyquist frequency using an approach similar to the RSI^2 algorithm. The method proposed is an output-driven process, where the stack is defined as a merge trace and has a potentially higher sampling rate than the input traces. Using this approach, the final stacked sections are not necessarily limited to the data-collected Nyquist frequencies.

Ronen (1987) justifies the possiblity of such recovery by posing the question of whether the information from different channels that are merged together during the process of stacking is redundant and also, whether summing is the optimal way to merge it. Figure 2.3 demonstrates that, if some independent filters are applied to a function before sampling, a certain amount of aliasing can be allowed, and one can recover the original signal. On the left is a schematic one-dimensional signal,

which is filtered by five analog-to-digital converters before sampling. The data are five different aliased sequences. The original signal cannot be recovered from any one sequence, but the combination of them may be sufficient. The same holds true for seismic data (Figure 2.4). Each trace of a CMP gather is limited by the Nyquist frequency. However, each offset corresponds to a different propagation path, so different information is attained. Therefore, the combination of all offsets allows us to reconstruct a higher frequency signal that is not necessarily limited by the Nyquist frequency of the input data traces. This is the fundamental principle of treating NMO and stack as an inverse process using shaping regularization to recover higher resolution stacks.

INVERSE NMO STACK USING SHAPING REGULARIZATION

In the proposed stacking methods in this thesis, I extend Claerbout's inverse NMO stack by implementing shaping regularization (Fomel, 2007) to provide additional constraints on the estimation result. In geophysical estimation problems, the estimated model is often ill-posed due to insufficient data, and small changes in the data result in drastic changes in the model. Regularization is used to solve ill-posed problems by providing additional constraints on the estimated model (Zhdanov, 2002). Shaping regularization is defined as a mapping of the input model to the space of acceptable functions. The mapping is controlled by the shaping operator, which is integrated in an iterative inversion. Iterative inversion repeatedly uses the difference between the estimated model from the current step and real data to update the model until convergence occurs (Ronen and Liner, 2000). In the linear case, the

solution of the estimation problem using shaping regularization is defined by:

$$\hat{\mathbf{m}} = [\mathbf{I} + \mathbf{S_m}(\mathbf{BF} - \mathbf{I})]^{-\mathbf{1}}\mathbf{S_m}\mathbf{Bd}, \tag{2.2}$$

where $\mathbf{F}$ is the forward operator, $\mathbf{B}$ is the backward operator, $\mathbf{S_m}$ is shaping regularization, and $\mathbf{d}$ is the input data. I implement the Generalized Minimum Residual (GMRES) algorithm to solve the linear system (Saad and Schultz, 1986). GMRES is a general iterative method for inverting sparse matrices.

In the context of NMO and stack, the model is a stack, and the data is a CMP gather (Figure 2.5). In the next two chapters, I define the operators $\mathbf{F}$, $\mathbf{B}$, and $\mathbf{S_m}$ used in shaping regularization for the shaping NMO and plane-wave construction (PWC) stacking methods. Both approaches compute NMO and stack in an iterative fashion using shaping regularization to achieve a higher resolution stack that avoids the effects of "NMO stretch".

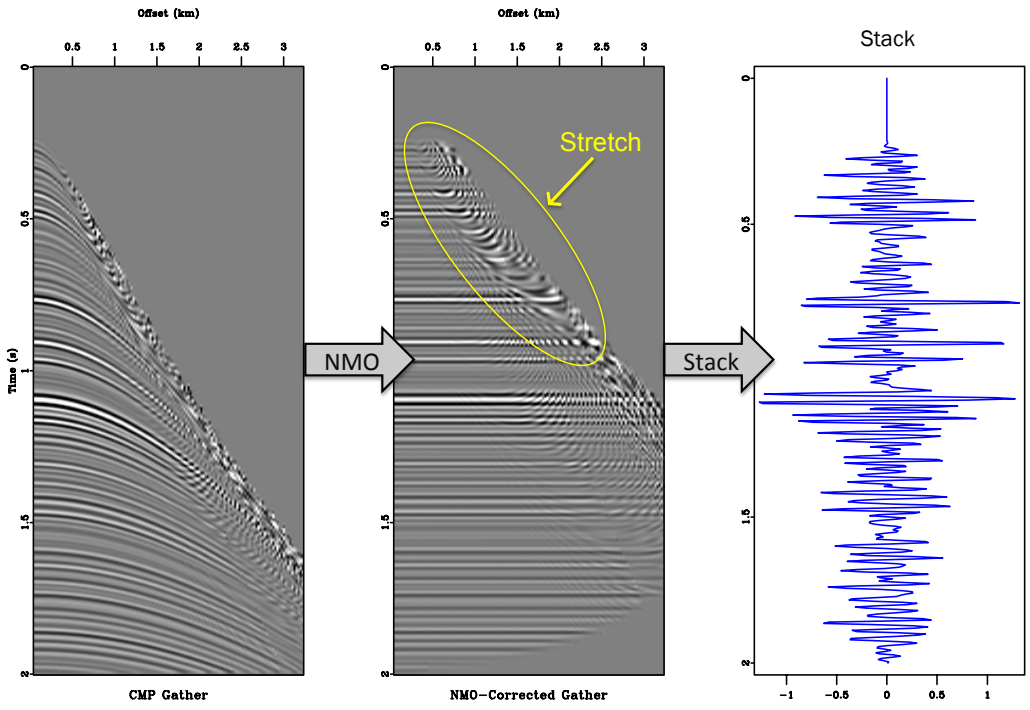

Figure 2.1: Synthetic example that demonstrates the process of NMO correction and stack. NMO and stack results in lower-amplitude and lower-resolution stacks due to distortions caused by "NMO stretch" if a stretch mute is not applied. ch02-review/. cmp2stack2

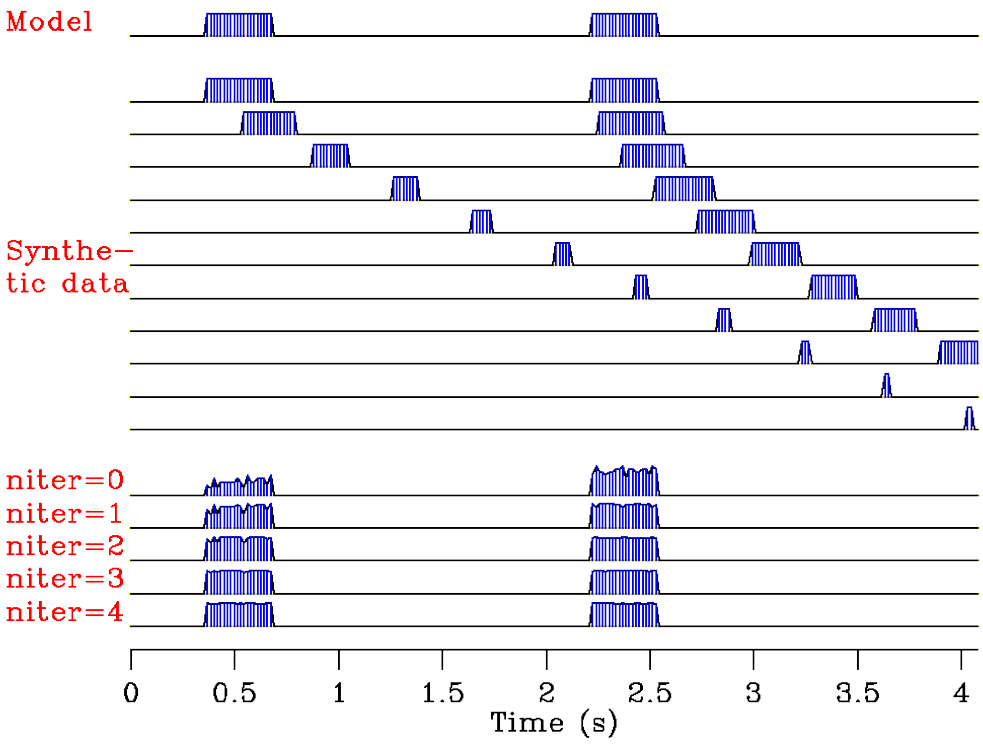

Figure 2.2: Inverse NMO stack example reproduced from Claerbout (1992). The model is a synthetic zero-offset trace and the data is a CMP gather. After just 4 conjugate gradient iterations, the waveform of the zero-offset trace is reconstructed. ch02-review/. invstck

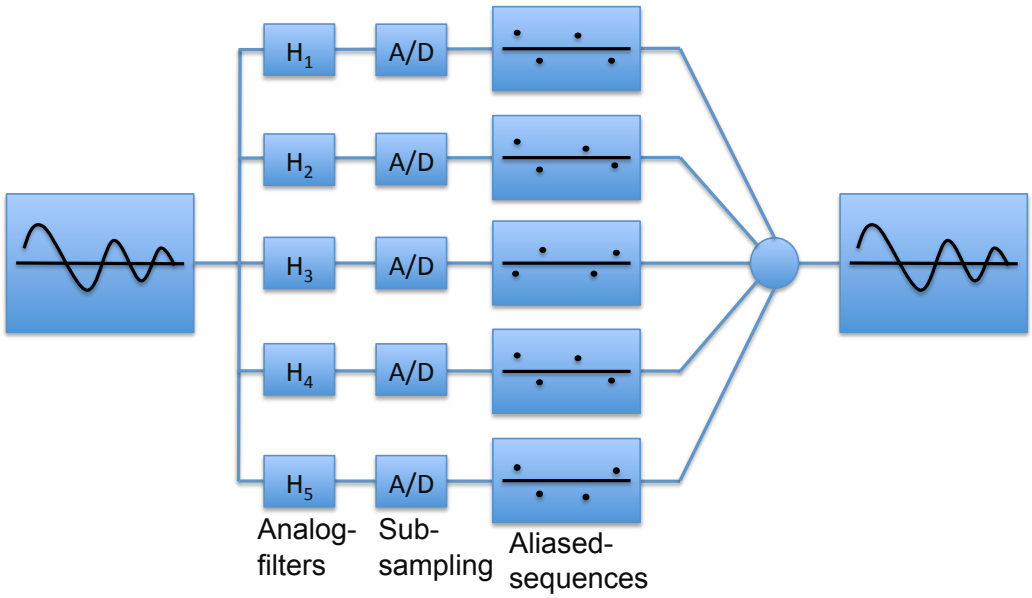

Figure 2.3: Figure reproduced from Ronen (1987). On the left is a one dimensional signal, which is filtered by five analog-to-digital converters before sampling. The data are five different aliased sequences. The original signal cannot be recovered from any one sequence but the combination of them might be sufficient. ch02-review/. ronen1

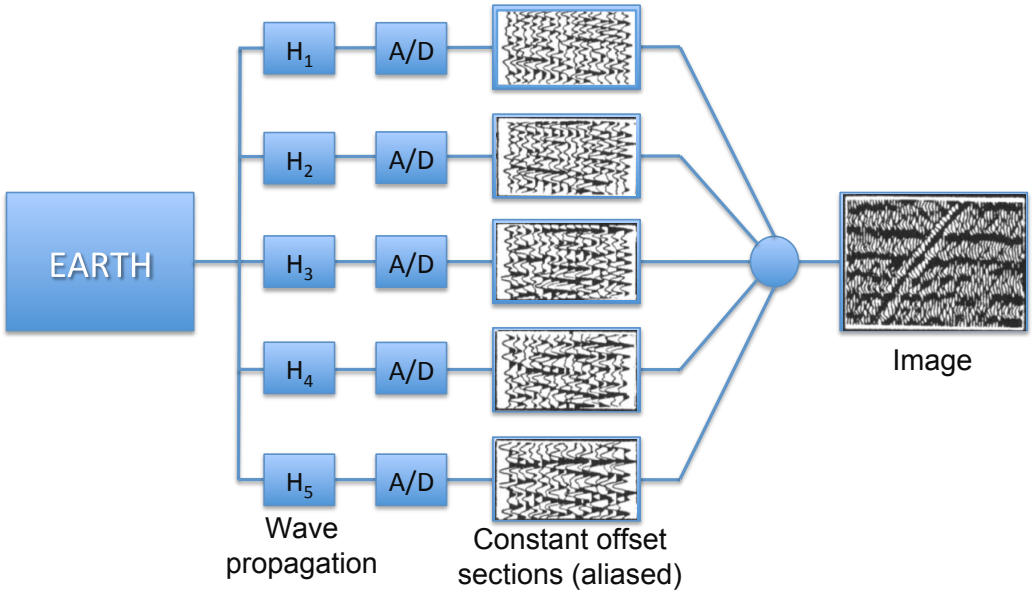

Figure 2.4: Figure reproduced from Ronen (1987). Each trace of a CMP gather is limited by the Nyquist frequency, but different offsets contain different wave propagation paths. When offsets are combined, there is potential to recover information that is higher frequency and not limited by the sampling rate of each individual trace. ch02-review/. ronen2

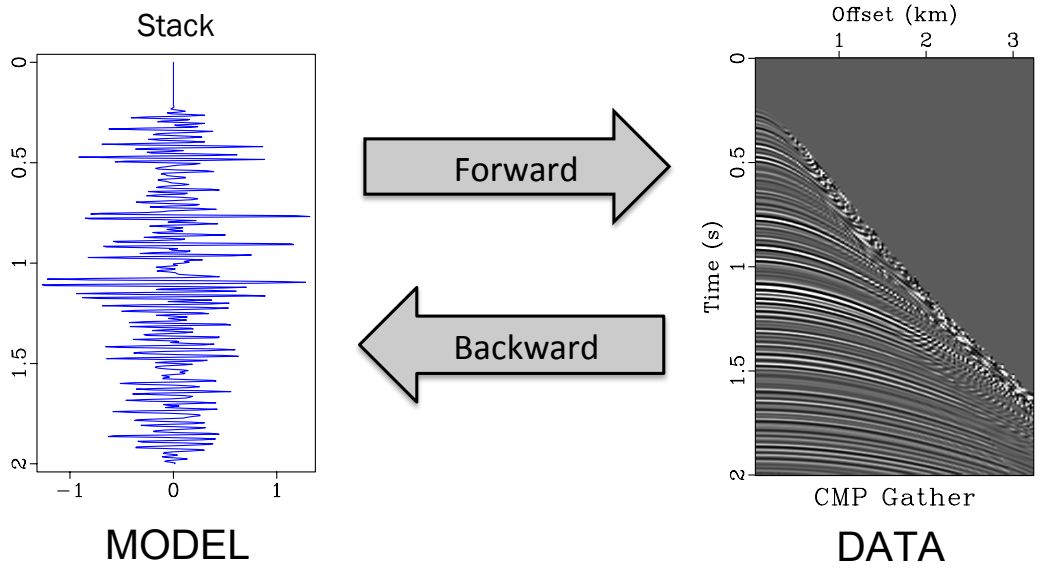

Figure 2.5: Schematic of treating NMO and stack as an inversion. The data space is a CMP gather, and the model space is a stack. The forward and backward operators are approximate inverses of each other. ch02-review/. shape2

Chapter 3

Shaping NMO stack

In this chapter, I present an alternative approach to the NMO-stack method that reduces the effects of "NMO stretch" by replacing conventional NMO and stack with a regularized inversion to zero offset. I use shaping regularization to achieve a stack that has a denser time sampling than the input and restores a wider frequency bandwidth compared with the conventional stack. In this application, the resulting stack is a model that best fits the data (CMP gather) using additional constraints imposed by shaping regularization. I start by reviewing shaping regularization and defining the operators in the context of NMO stack. Numerical tests demonstrate that "stretching effects" caused by NMO correction are reduced, and the frequency content of the true zero-offset trace is accurately reconstructed.

METHOD

In geophysical estimation problems, regularization is used to solve ill-posed problems by providing additional constraints on the estimated model. Shaping regularization (Fomel, 2007, 2008) implies a mapping of the input model $\mathbf{m}$ to the space of acceptable functions. The mapping is controlled by the shaping operator $\mathbf{S_m}$, which is integrated in an iterative inversion algorithm. Iterative inversion repeatedly uses the difference between the estimated model from the current step and real data to update the model until convergence occurs (Ronen and Liner, 2000). In the linear

case, the solution of the estimation problem using shaping regularization is defined as (Fomel, 2007):

$$\hat{\mathbf{m}} = [\mathbf{I} + \mathbf{S_m}(\mathbf{BF} - \mathbf{I})]^{-\mathbf{1}}\mathbf{S_m}\mathbf{Bd}, \tag{3.1}$$

where $\mathbf{F}$ is the forward operator, $\mathbf{B}$ is the backward operator, and $\mathbf{d}$ is the input data. I implement the Generalized Minimum Residual (GMRES) algorithm (Saad and Schultz, 1986) to perform the linear inversion in equation 3.1.

The main idea of shaping regularization in application to NMO stack is to use signal from different offsets to recover extra bandwidth in the zero-offset trace. In conventional NMO correction, different estimates of the zero-offset trace from the data recorded at different offsets might have different spectral bands due to NMO stretch (Claerbout, 1996). At long offsets, low frequencies exist, which extend the spectral bandwidth. There is interest in the search for both high and low frequencies.

I start by defining vectors and linear operators used in this formulation as follows:

- $\mathbf{m}$ (model) is the desired seismic trace at zero-offset.
- $\mathbf{d}$ (data) is a CMP gather.
- $\mathbf{F}$ (forward operator) applies inverse moveout by spraying along hyperbolas using a known velocity model and subsamples in time (Figure 3.1).
- $\mathbf{B}$ (backward operator) interpolates the data to a denser temporal grid and applies NMO correction and stack (Figure 3.2).
- $\mathbf{S_m}$ (shaping operator) is a bandpass filter.

The estimation result is controlled by the shaping operator. Therefore, the estimated stack is sensitive to how the bandpass filter $\mathbf{S_m}$ is defined. The bounds of the bandpass operator depend on the range of frequencies that exist in the data and, hence, are unique to the dataset.

SYNTHETIC EXPERIMENTS

High frequency recovery

I evaluate the performance of shaping NMO stack by applying it to synthetic data and comparing the results to conventional NMO and stack. In the first experiment, a synthetic trace was generated with a sampling interval of 1 ms and was used as a reference trace. This trace was then inverse NMO-corrected and subsampled to 4 ms to produce a CMP gather, shown in Figure 3.3, which is the input data for both shaping and conventional NMO and stack methods. The convergence of the GMRES algorithm in this example required 5 iterations to achieve a relative misfit tolerance of 10^{-5}. Figure 3.4 shows the shaping NMO stack as a function of iteration. Iteration 0 is similar to conventional NMO and stack, and iteration 5 is the estimation result, where frequency content and amplitude appear to be noticeably higher. The stack produced using shaping NMO is compared with the reference trace and the conventional stack in Figure 3.5. There appear to be minimal differences in amplitude and frequency content between the reference trace and the shaping NMO stack. Compared to conventional NMO and stack, higher frequencies and amplitudes exist throughout the stack. I next evaluated the spectral content of each stack compared to the reference trace. The frequency spectrum of the stacked trace produced using shaping NMO stack is compared with that of the conventional stack in Figure 3.6(a) and the reference trace in Figure 3.6(b). Figure 3.6(a) shows that the conventional

stack fails to recover useful frequencies ranging from 110 Hz to 175 Hz. The shaping stack spectrum contains higher frequencies, ranging to approximately 175 Hz. To demonstrate that the recovered high frequencies are accurate, I compare the spectrum of the reference trace to that of the shaping NMO stack, which results in a nearly perfect match (Figure 3.6(b)). This demonstrates that the true-amplitude scale and spectrum of the reference trace is accurately recovered by using inversion. In this simple synthetic example, by implementing shaping regularization, I accurately preserve information in the recovered zero-offset trace with a 1 ms sampling interval by using input data with only a 4 ms sampling interval.

To add complexity to the synthetic CMP gather, I incorporate the effects of random noise (Figure 3.7) and apply shaping NMO stack and conventional NMO and stack. A spectral comparison of the resulting estimated stack after apply shaping NMO stack versus conventional NMO and stack is shown in Figure 3.8(a) and the reference trace in Figure 3.8(b). The shaping NMO stack still achieves higher frequency content than the conventional stack that is consistent with the reference trace. The frequency content recovered using shaping regularization is not altered by adding random noise to the data. This is to be expected due to the power of conventional stacking. I next add artificial AVO effects to the CMP gather, where amplitude decreases linearly with offset, shown in Figure 3.9. The resulting spectral comparisons are shown in Figure 3.10. In Figure 3.10(a), the shaping stack still recovers higher frequency content in comparison to conventional NMO and stack. When comparing the shaping stack spectrum to that of the reference trace in Figure 3.10(b), there is a mismatch in amplitude due to the decrease in energy of the input gather, but the same spectral content as the reference trace is still achieved. Therefore, by adding in the complexities of random noise and AVO effects, shaping NMO stack accurately

recovers high frequencies present in the reference trace. Conventional AVO methods are done through weighted stacking (Smith and Gidlow, 1987) to display information about rock properties. Therefore, the principles of shaping NMO stack can be extended to the application of AVO analysis to compute high resolution weighted stacks.

Low frequency recovery

Low frequencies play an important role in seismic inversion for velocity and impedance models (Kroode et al., 2013). I next evaluate the ability of the algorithm to recover low-frequency information in the estimated stack. I apply a low-cut filter to the synthetic CMP gather in order to remove all of the useful low frequencies below 25 Hz (Figure 3.11), which is the input for shaping NMO stack and conventional NMO and stack. A spectral comparison of the estimated stack to conventional NMO and stack and the reference trace are shown in Figure 3.12. I zoom in to the low end of the frequency spectrum to see how well each method does in comparison to the reference trace, displayed in Figure 3.13. Conventional NMO and stack fails to recover frequencies below 25 Hz, while shaping NMO stack recovers more low-frequency information that are consistent with the reference trace. This indicates that shaping NMO stack is capable of recovering lower frequencies as well as higher frequencies compared to the conventional stacking approach.

"Non-stretch" NMO example

To demonstrate how shaping NMO stack reduces the effects of "NMO stretch", I make use of the linearity of the shaping NMO operator and apply it to each trace of the CMP gather, setting the rest of the gather to zero. After repeating this process

for all traces in the gather, the output shaping stacks are concatenated to extract the effective NMO-corrected gather. Figure 3.14 compares the conventional NMO-corrected gather with and without a stretch mute to the effective NMO-corrected gather using shaping NMO stack. The results indicate that the "stretching" effects that are prominent at far offsets and early times in the conventional NMO-corrected gather without a stretch mute are effectively reduced by implementing the shaping stack approach.

CONCLUSIONS

Conventional NMO stack may result in lower resolution stacked sections due to distortions caused by NMO correction and stretch muting. Treating the process of NMO stack as a regularized inversion allows us to compute the optimal stack with higher frequency content. Shaping regularization adds additional constraints, namely a bandpass filter, to provide control on the estimated stack. Numerical tests demonstrate the ability of shaping NMO stack to recover both higher and lower frequencies in comparison with conventional NMO stack. By implementing shaping NMO stack, signal from different offsets is effectively utilized and the effects of "NMO stretch" are minimized to recover extra bandwidth in the optimized stack. The results can aid in imaging and interpretation of small-scale features such as thin layers and diffractions.

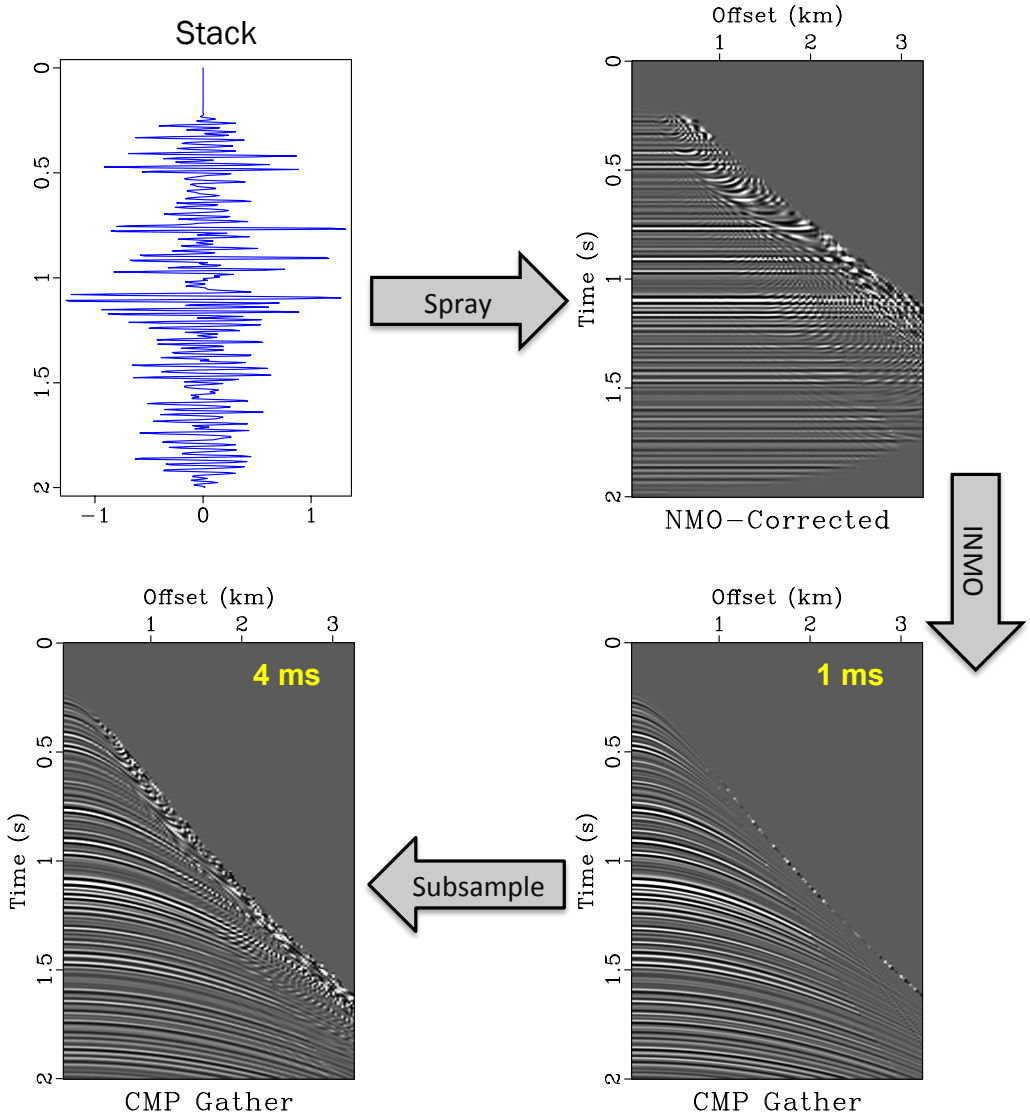

Figure 3.1: Schematic example of the forward operator in shaping regularization going from the model space (stack) to the data space (CMP gather). The forward operator consisted of three steps: spray the stack to all offsets, inverse NMO correction, and subsample to a sparser grid (1 ms to 4 ms). ch03-shstack/. shForward

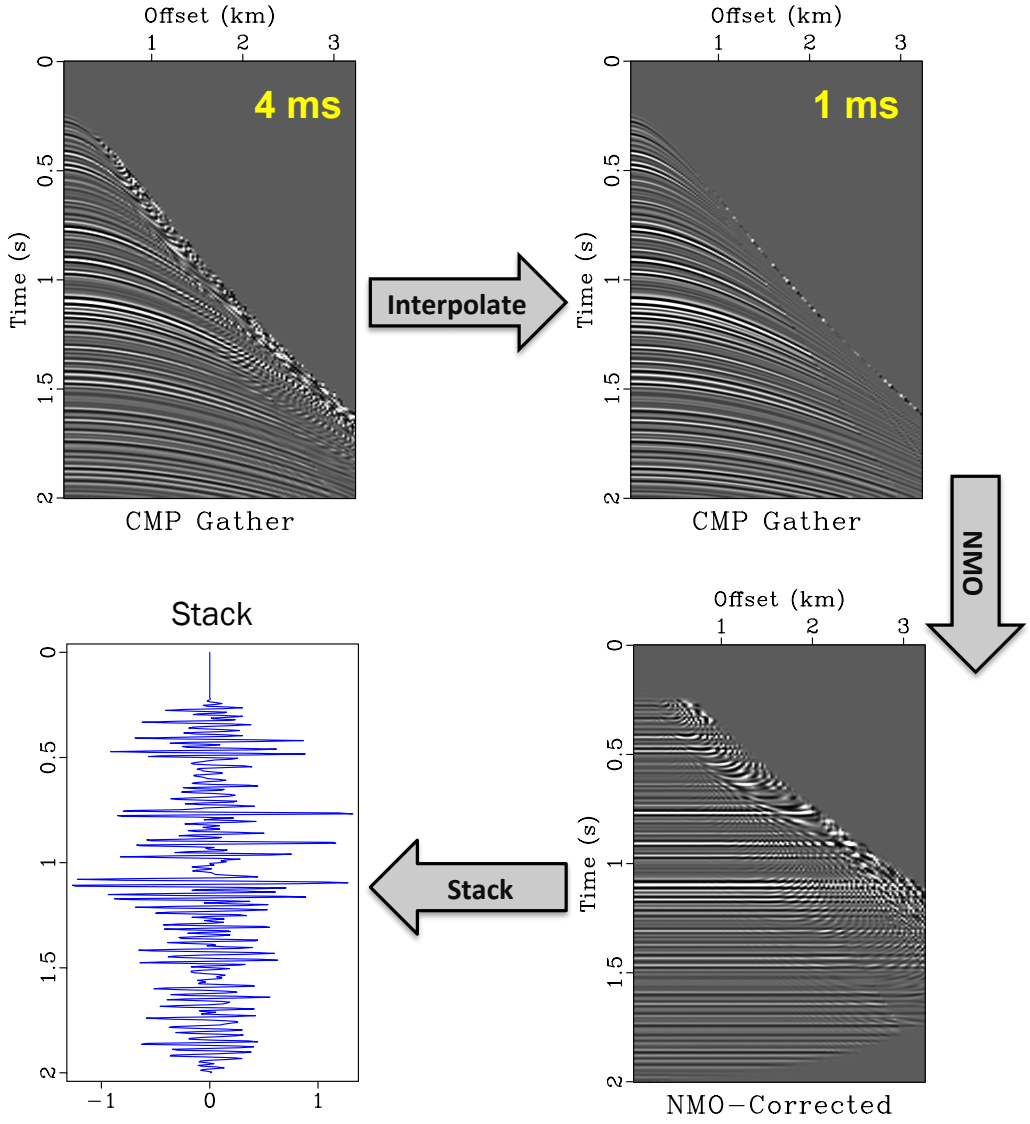

Figure 3.2: Schematic example of the backward operator in shaping regularization going from the data space (CMP gather) to the model space (stack). The backward operator is comprised of three main steps: spline interpolation to a denser grid (4 ms to 1 ms), NMO correction and stack. ch03-shstack/. shBackward

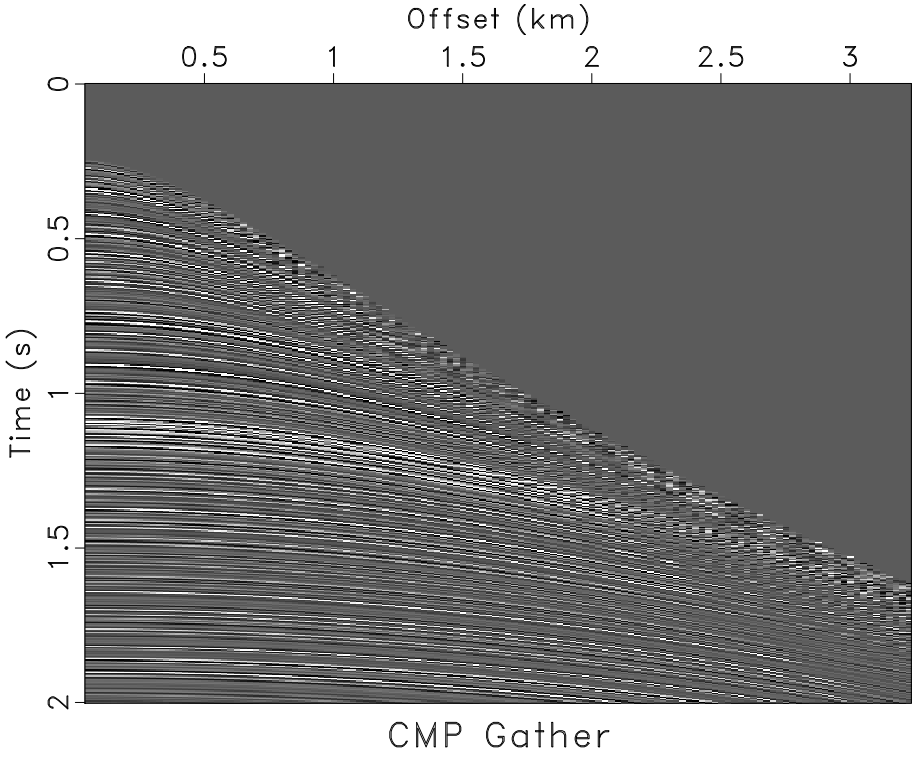

Figure 3.3: Synthetic CMP gather with a 4-ms sampling interval used as the input data for shaping NMO stack and conventional NMO stack. ch03-shstack/synthetic shcmp2

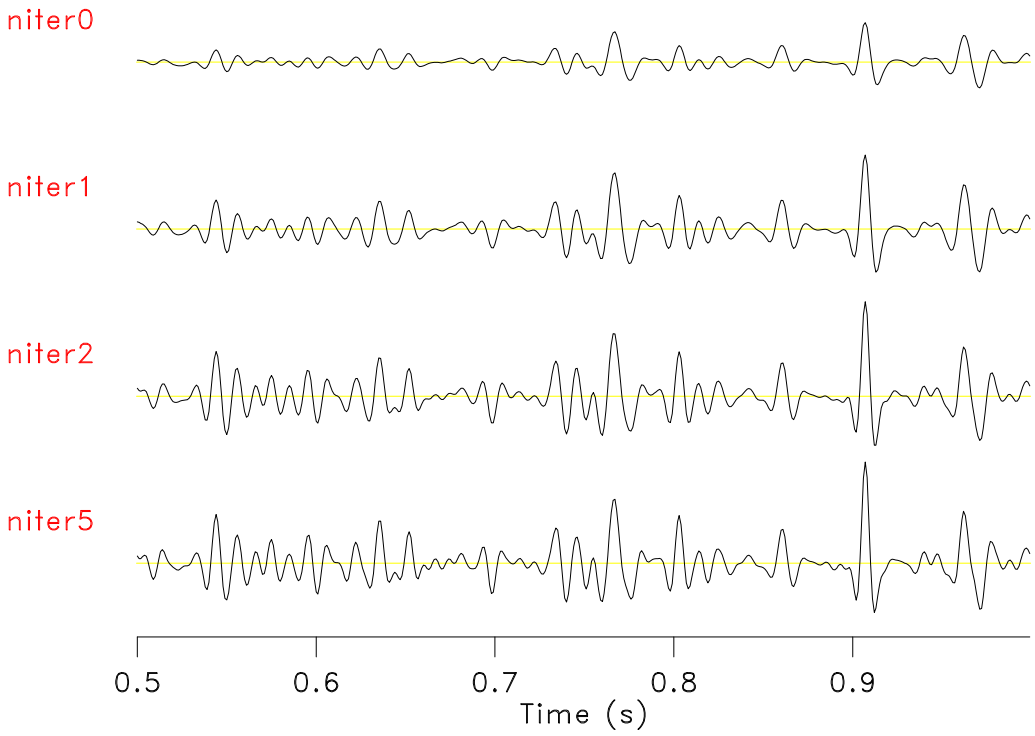

Figure 3.4: Zoomed in portion of the estimated stack as a function of iteration using shaping regularization. Iteration 0 is similar to conventional NMO and stack, and iteration 5 is the estimation result, where frequency content and amplitude appear to be noticeably higher. ch03-shstack/synthetic shmod1

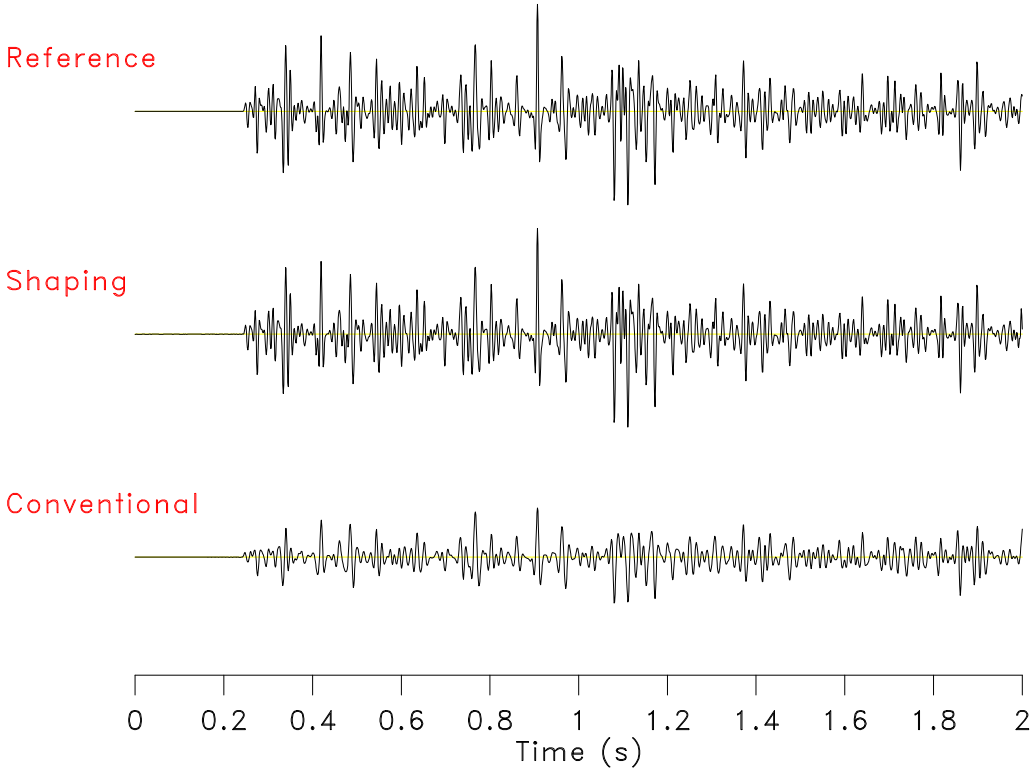

Figure 3.5: Comparison of the resulting shaping NMO stack and conventional stack to the zero-offset reference trace. ch03-shstack/synthetic shmod3

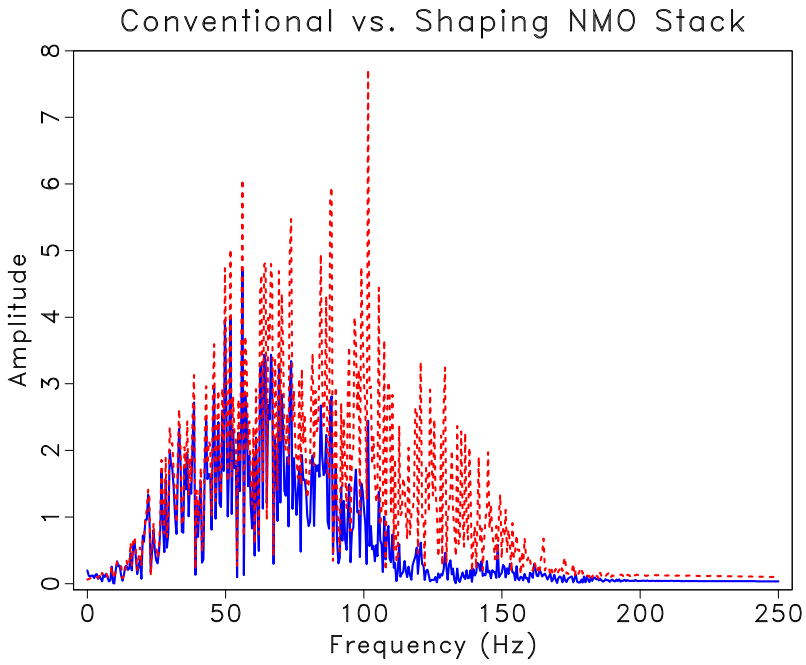

(a)

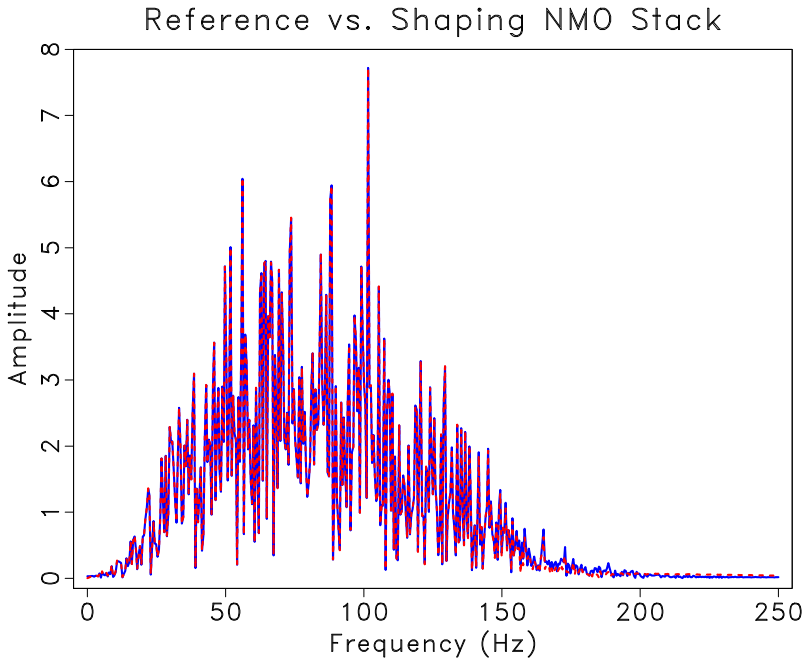

(b)

Figure 3.6: Spectral comparison of the shaping NMO stack (dashed red) with (a) conventional NMO and stack (blue) and (b) the reference trace (blue) with a 1-ms sampling interval. ch03-shstack/synthetic shspec5,shspec6

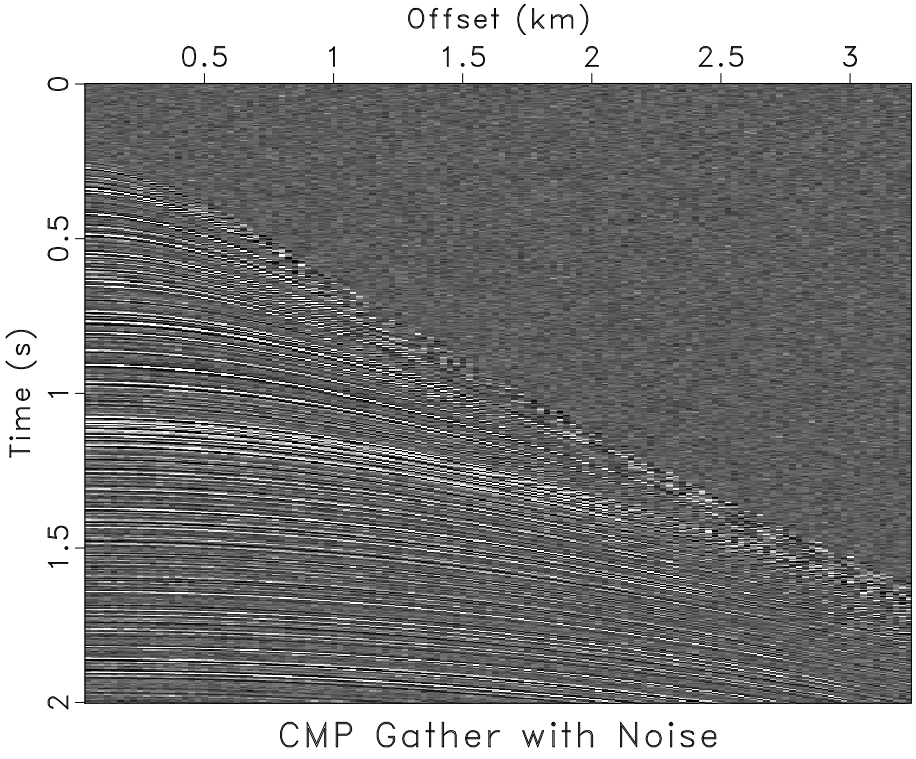

Figure 3.7: Synthetic CMP gather with random noise, which is used as the input data for shaping NMO stack and conventional NMO stack. ch03-shstack/synthetic shcmpnoise

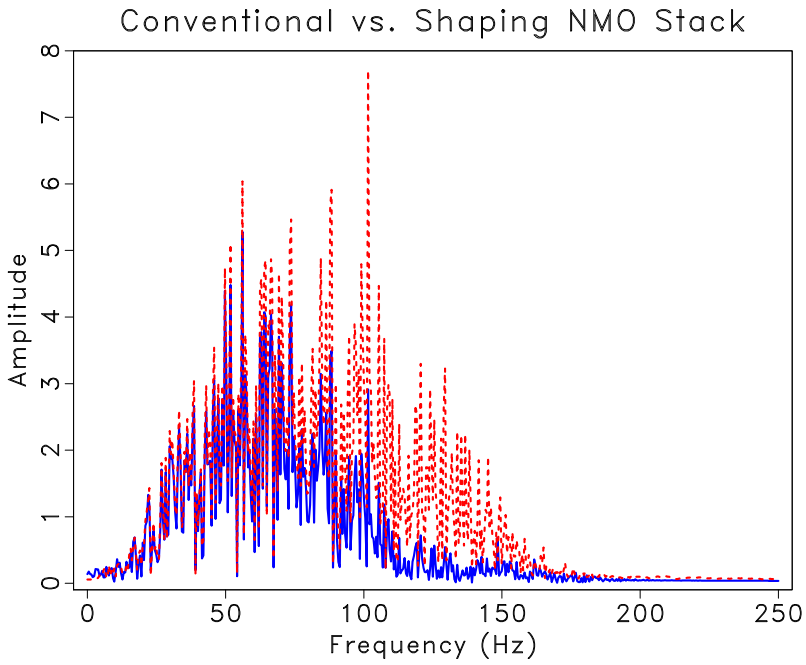

(a)

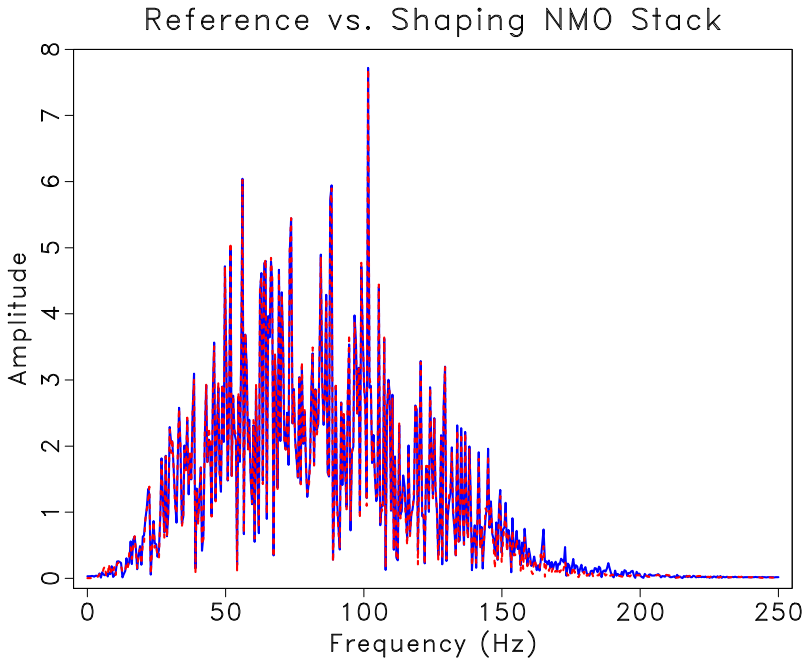

(b)

Figure 3.8: Resulting spectral comparisons of stacks with random noise applied to input data. Spectrum of the shaping NMO stack (dashed red) vs. (a) spectrum of conventional stack (blue) and (b) spectrum of reference trace (blue) with 1-ms sampling interval. ch03-shstack/synthetic shspecnoise2,shspecnoise1

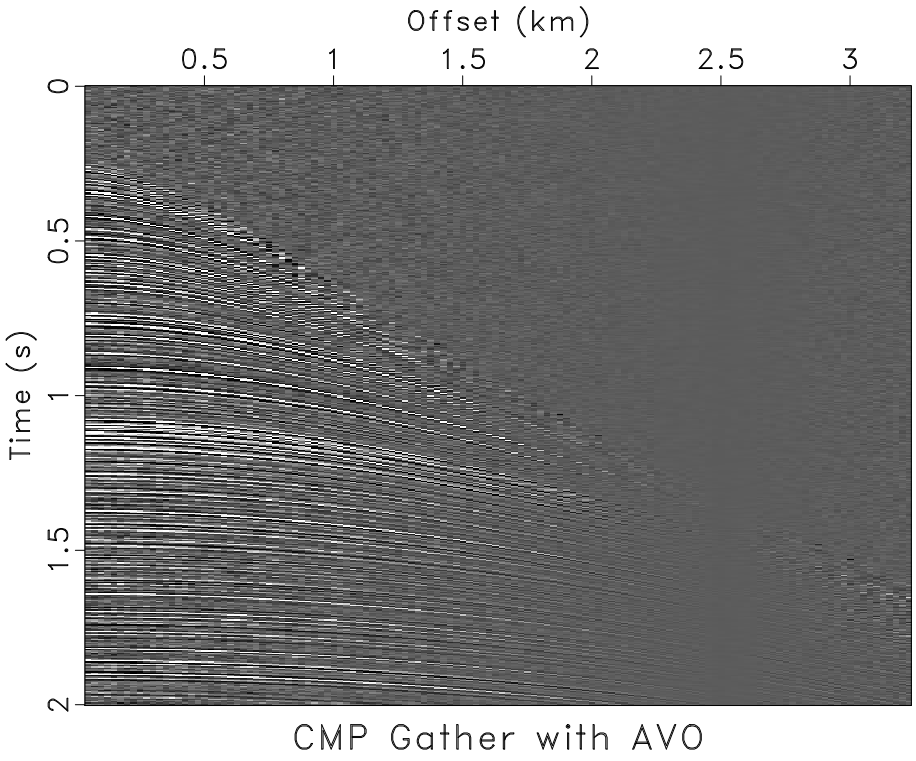

Figure 3.9: Synthetic CMP gather with random noise and artificial AVO effects, where amplitude decreases with offset. ch03-shstack/synthetic shcmpavo

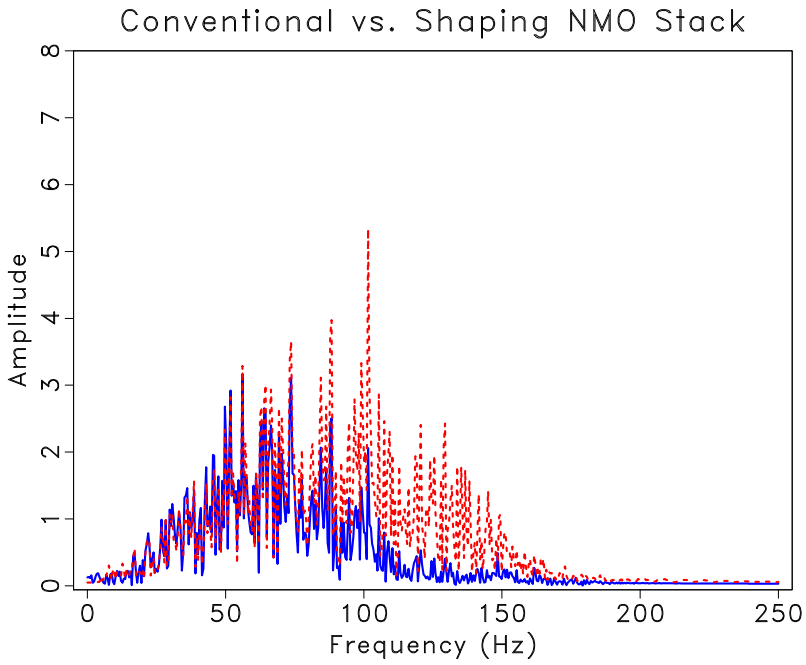

(a)

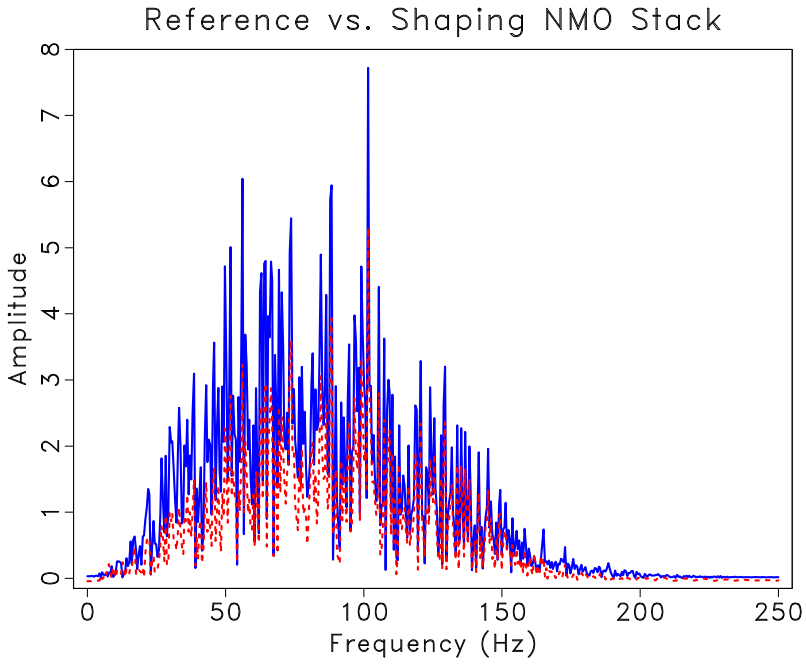

(b)

Figure 3.10: Spectral comparison of resulting stacks with random noise and AVO effects applied to input data. Spectrum of the shaping NMO stack (dashed red) vs. (a) conventional NMO and stack (blue) and (b) the reference trace (blue) with a 1-ms sampling interval. ch03-shstack/synthetic shspecavo2,shspecavo1

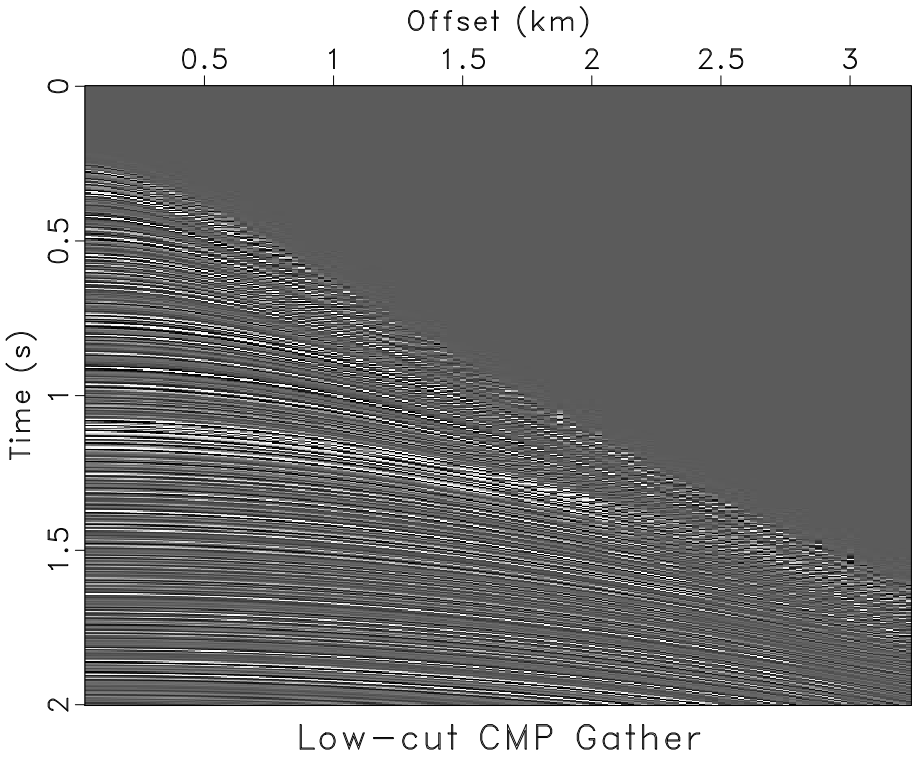

Figure 3.11: Synthetic CMP gather with a low-cut filter applied, cutting out all frequencies below 25 Hz. ch03-shstack/synthetic shcmplow

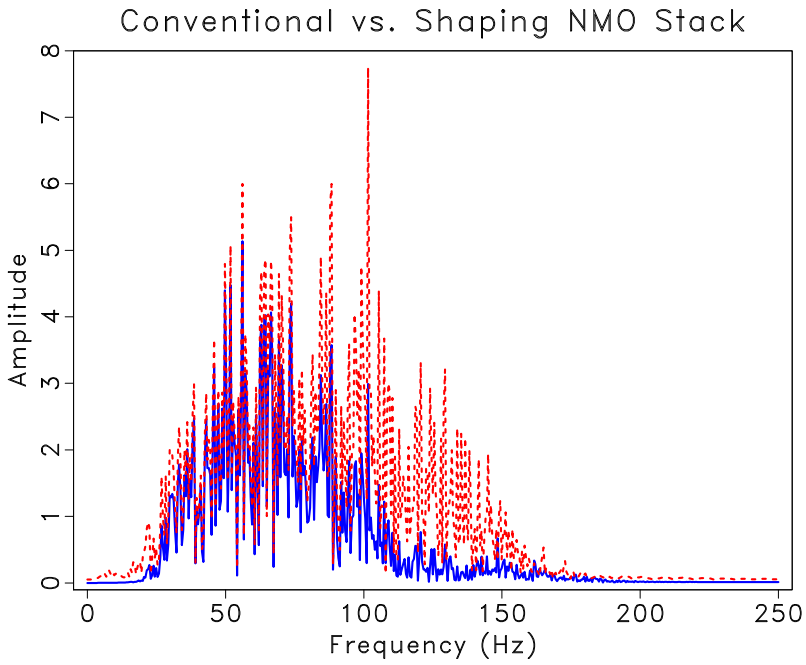

(a)

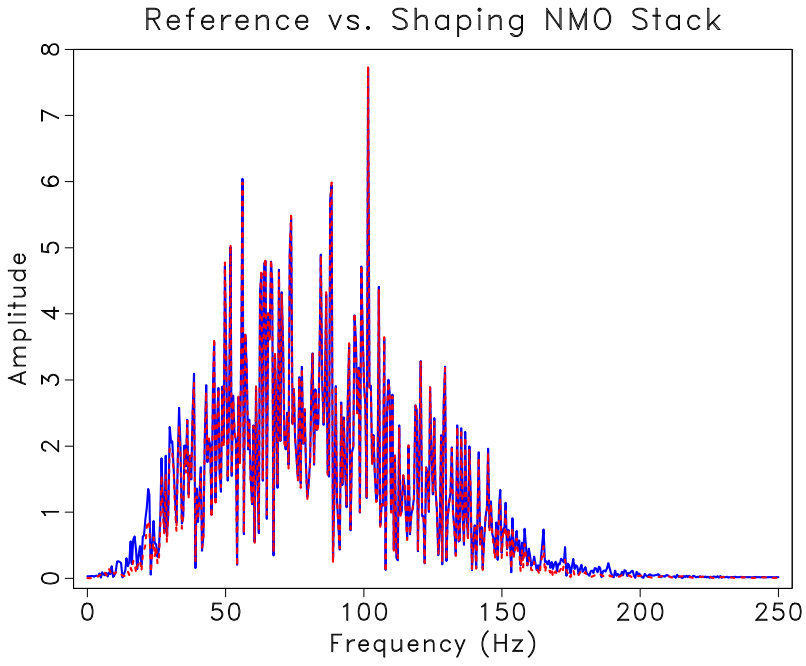

(b)

Figure 3.12: Spectral comparison of resulting stacks with a low-cut filter applied to input data. Spectrum of the shaping NMO stack (dashed red) with (a) conventional NMO and stack (blue) and (b) the reference trace (blue) with a 1-ms sampling interval. ch03-shstack/synthetic shspeclow2,shspeclow1

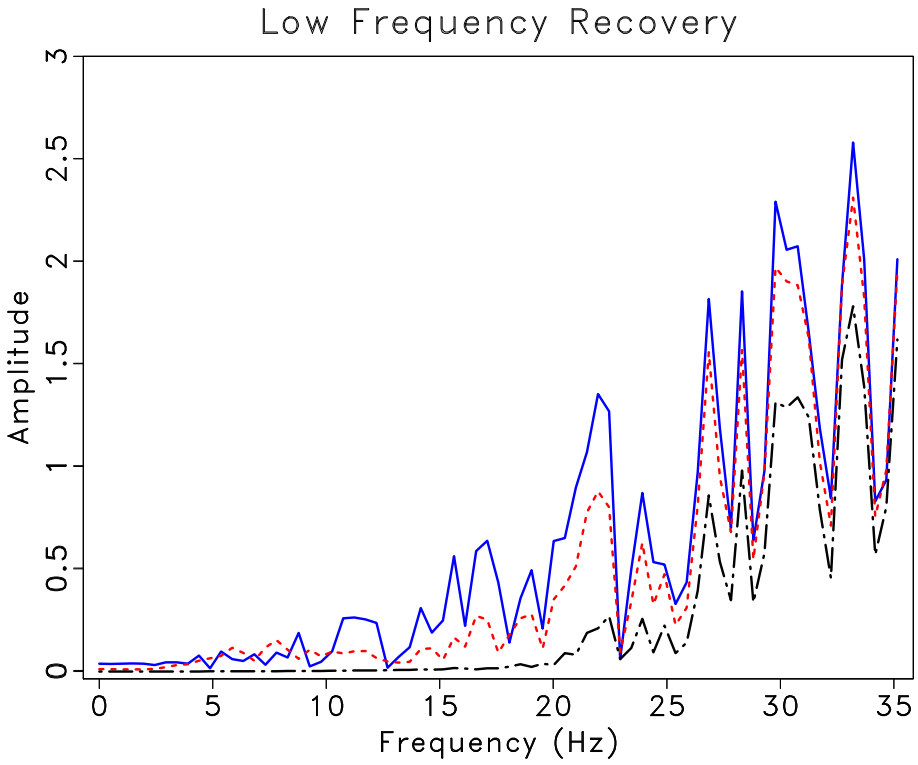

Figure 3.13: Spectral comparison of the low frequencies recovered. Shaping NMO stack (dashed red) recovers lower frequencies in comparison with the conventional stack (dot-dash black) and is consistent with the reference trace (blue). ch03-shstack/synthetic shspeclow3

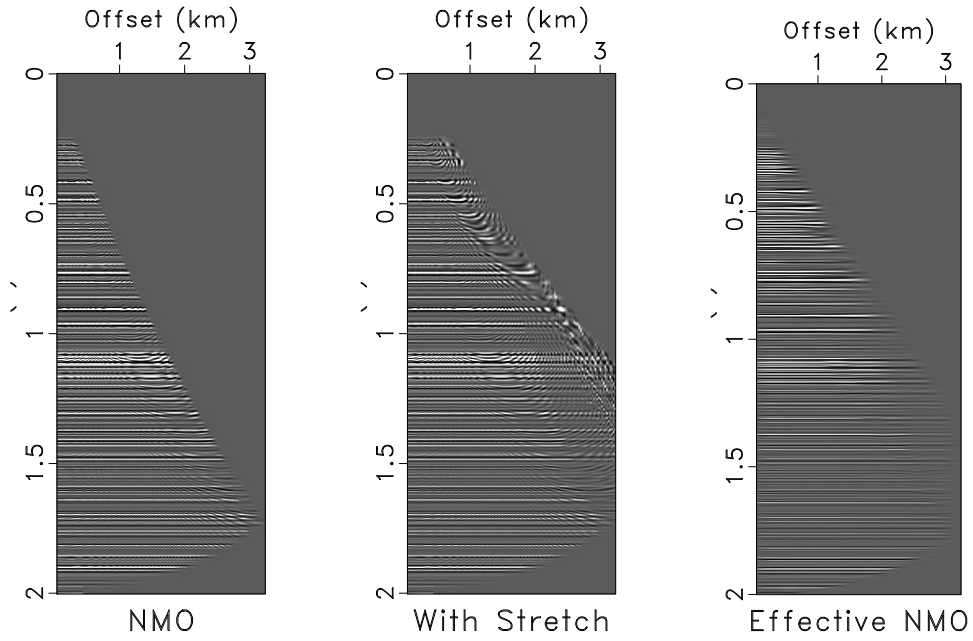

(a) (b) (c)

Figure 3.14: (a) Conventional NMO correction, (b) NMO correction without stretch muting and (c) effective NMO correction using shaping NMO stack on each trace of the CMP gather to demonstrate non-stretch NMO. ch03-shstack/synthetic shnmo3,shnmo2,shnsnmo

Chapter 4

Recursive stacking using plane-wave construction

In this chapter, I propose an alternative approach to normal moveout (NMO) stacking that eliminates the effects of "NMO stretch" and restores a wider frequency band by replacing conventional stacking with a regularized inversion to zero offset. The resulting stack is a model that best fits the data using additional constraints imposed by shaping regularization. I extend the method of shaping NMO stack from chapter 3 further by introducing a recursive stacking scheme using plane-wave construction (Fomel and Guitton, 2006) in the backward operator of shaping regularization to achieve a higher resolution stack. The advantages of using recursive stacking along local slopes in the application to NMO and stack is that (1) it avoids "stretching effects" caused by NMO correction and (2) is insensitive to non-hyperbolic moveout in the data. Numerical tests demonstrate the algorithm's ability to attain a higher frequency stack with a denser temporal sampling interval compared to those of the conventional stack and to minimize stretching effects caused by NMO correction. The synthetic results are compared with those of the shaping NMO stack from chapter 3.

METHOD

Shaping regularization in the application to NMO stack utilizes signal from different offsets to reconstruct a high-resolution stack. The model $\mathbf{m}$ is in this case a seismic trace at zero-offset and the data $\mathbf{d}$ is a CMP gather. I define the linear

operators used in the shaping regularization scheme in equation 3.1 as:

- **F** (forward operator) applies predictive painting (Fomel, 2010) to spread information using a known dip field and then subsamples in time (Figure 4.2).
- **B** (backward operator) interpolates the data in time to a denser grid and stacks in a recursive fashion using local slopes (Figure 4.3).
- $\mathbf{S_m}$ (shaping operator) is a bandpass filter that controls frequency content.

I implement PWC stacking in the backward operator of shaping regularization which follows local-slope calculations from a CMP gather. The key idea of this stacking procedure is to start at the farthest offset trace of the gather and make a local slope prediction of the preceding trace using PWC (Figure 4.1a). The partially corrected trace is then stacked with the uncorrected neighbor, which is the input for the next local prediction (Figure 4.1b). The process is repeated in the offset direction until the near-offset trace is reconstructed (Figure 4.1c). The final step to this stacking scheme is to apply a near-offset NMO correction to reconstruct the zero-offset trace. This recursive stacking approach results in higher resolution stacks compared to conventional NMO and stack. The procedure is equivalent to computing the zero scale of the seislet transform (Fomel and Liu, 2010). Advantages of PWC stacking include eliminating the effects of "NMO stretch" as well as the problem of non-hyperbolic moveout. The approximate inverse of PWC stacking is defined by predictive painting (Fomel, 2010). This algorithm is comprised of two main steps, namely estimating local slopes of seismic events using plane-wave destruction (PWD) (Fomel, 2002) and spreading information from a seed trace inside a volume. To implement the forward operator **F**, I use the updated model to spread information across the CMP gather using the estimated dip field.

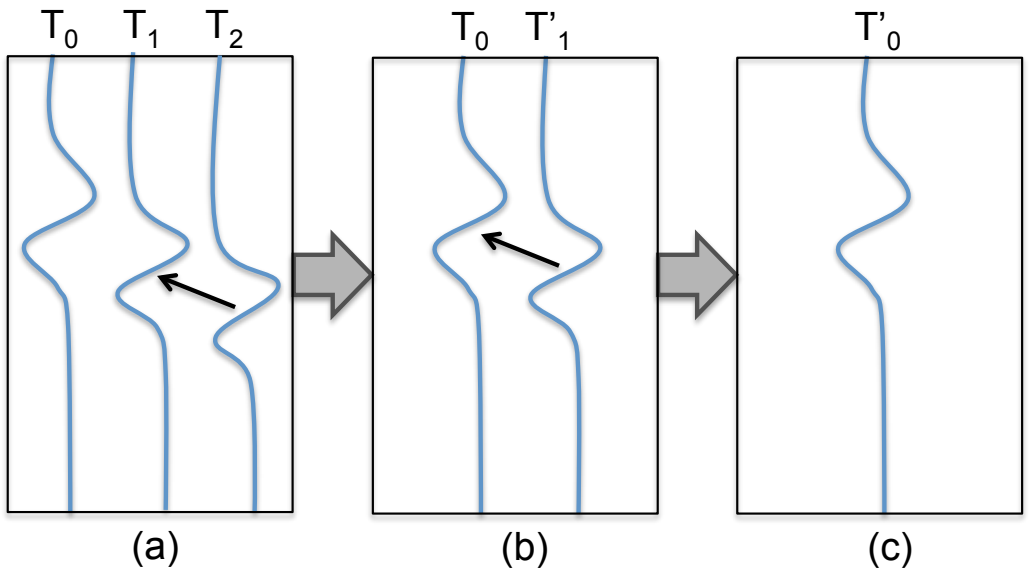

Figure 4.1: Schematic of PWC stacking algorithm. (a) Stack far offset trace T_2 with neighboring trace T_1, (b) stack updated trace T'_1 with neighboring trace T_0, (c) accumulated near-offset stack. ch04-shseislet/ schematic

In PWC stacking, each seismic trace is predicted from its neighbors that are shifted along the event slopes. Slopes are estimated by PWD, which minimizes the prediction error to estimate optimal slopes. PWD can be sensitive to conflicting slopes at far offsets of a CMP gather where the dips are large. This can cause PWC stacking to fail in characterizing an optimal stack. To account for this issue, I first apply a constant velocity NMO correction to the CMP gather, which results in smoothly varying slopes without crossing events. I then estimate the moveout $t(x)$ of the corrected seismic events at offset x as follows:

$$t(x) = \sqrt{t_0^2 + \frac{x^2}{v_0^2} + x^2 \left(\frac{1}{v^2} - \frac{1}{v_0^2} \right)}, \tag{4.1}$$

where t_0 is the zero offset travel-time, v is the NMO velocity estimated by a conventional method and v_0 is a constant velocity. Figure 4.4 displays the approximated

moveout of the constant velocity NMO-corrected gather. Adding the correction factor due to the constant velocity NMO correction from equation 4.1, the dip field becomes:

$$p = \frac{x}{t}\left(\frac{1}{v^2} - \frac{1}{v_0^2}\right). \tag{4.2}$$

I use this estimated dip as the initial model for PWD. This dip estimation scheme follows the velocity-dependent formulation of the seislet transform (Liu et al., 2015) and provides a better estimation of the dip field for CMP gathers with large dipping events and conflicting slopes at far offsets. I incorporate this dip estimation method to compute the PWC stack in an iterative fashion while using shaping regularization (equation 3.1).

SYNTHETIC EXPERIMENTS

In the first synthetic experiment, I generated a synthetic trace with a sampling interval of 1 ms and used it as a reference trace. This trace was then inverse NMO-corrected and subsampled to 4 ms to produce a CMP gather (Figure 4.5(a)), which became the input data for PWC stack and conventional NMO and stack. The result of applying a constant velocity NMO correction is displayed in Figure 4.5(b) and is used to compute the dip field.

High frequency recovery

The convergence of the GMRES algorithm in this example required only 3 iterations to achieve a misfit tolerance of 10^{-5}. The estimated PWC stack is shown in Figure 4.6 as a function of iteration, where iteration 0 is the initial model and iteration 3 is the final estimation result using PWC stacking. The conventional stack results in lower amplitude and lower frequency content, while the PWC stack achieves results

similar to the reference trace (Figure 4.7). I next compare the frequency content of the PWC stack with the conventional stack (Figure 4.8(a)) and the reference trace (Figure 4.8(b)). The conventional stack fails to recover useful frequencies ranging from 110 Hz to 175 Hz, whereas the PWC stack contains frequencies up to 175 Hz. Using inversion, I accurately preserve the true amplitude scale and spectrum of the reference trace. One notable observation is that the high frequency information recovered is beyond the Nyquist frequency of the input data (125 Hz).

To add complexity to the synthetic CMP gather, I incorporate random noise (Figure 4.9) and apply PWC stack and conventional NMO and stack. A spectral comparison of the PWC stack versus conventional NMO and stack is shown in Figure 4.10(a) and the reference trace in Figure 4.10(b). The frequency content recovered using shaping regularization does not change by adding random noise to the data. I next add artificial AVO effects to the CMP gather (Figure 4.11), where amplitude is linearly decreasing with offset. The resulting spectral comparisons are shown in Figure 4.12. In Figure 4.12(a), the PWC stack still recovers higher frequency content in comparison to conventional NMO and stack. When comparing the spectral band of the PWC stack to that of the reference trace in Figure 4.12(b), the difference is minimal. Therefore, by adding the complexities of artificial AVO effects and random noise to the synthetic data, the ability of PWC stack to reconstruct the zero-offset trace was not affected, whereas the frequency content recovered by the conventional stack is limited to the sampling rate of the input data and also the problems that arise with the assumptions of conventional CMP stacking.

Low frequency recovery

Low frequencies play an important role in seismic inversion for velocity and impedance models (Kroode et al., 2013). I next evaluate the algorithm's ability to recover low frequency information in the estimated stack. I apply a low cut filter to the synthetic CMP gather to remove all of the useful low frequencies below 25 Hz. A spectral comparison of the resulting PWC stack to conventional NMO stack and the reference trace is shown in Figure 4.14. I zoom in to the low end of the frequency spectrum to see how well each method does in comparison to the reference trace, which is shown in Figure 4.15. Conventional NMO stack fails to recover frequencies below 25 Hz, while the PWC stack recovers more low frequency information that is consistent with the reference trace.

"Non-stretch" NMO

To demonstrate how PWC stacking reduces the effects of "NMO stretch", I apply this method to each trace of the CMP gather, setting other traces to zero. After repeating this process for all traces in the gather, the output PWC stacks are concatenated to extract the effective NMO-corrected gather. Figure 4.16(a) displays the conventional NMO-corrected gather with a stretch mute applied, where far offset information is lost. Figures 4.16(b) and 4.16(c) compare the NMO-corrected gather before stretch muting to the effective NMO-corrected gather using PWC stacking. The results indicate that the stretching effects that are prominent at far offsets and early times in the NMO-corrected gather without a stretch mute are effectively reduced by implementing PWC stack.

CONCLUSIONS

Conventional NMO stack may result in lower resolution stacked sections due to distortions caused by NMO correction and stretch muting. Treating the process of NMO and stack as a regularized inversion allows us to compute an optimal stack with higher frequency content. Low frequency content also plays an important role in seismic data processing and imaging. As demonstrated by the numerical examples, PWC stacking has the ability to recover both higher and lower frequencies compared to conventional NMO and stack. Furthermore, by adding artificial AVO effects and random noise to the data, PWC stack still has the ability to preserve the true amplitude scale and spectrum of the reference trace. The shaping NMO stack in chapter 3 is capable of recovering lower frequency content than the PWC stack. However, advantages of the PWC stack include the insensitivity to non-hyperbolic moveout and AVO effects, as well as its ability to converge in fewer iterations in comparison with the shaping NMO stack. By implementing PWC stack, resolution is gained by utilizing signal from different offsets and minimizing stretching effects.

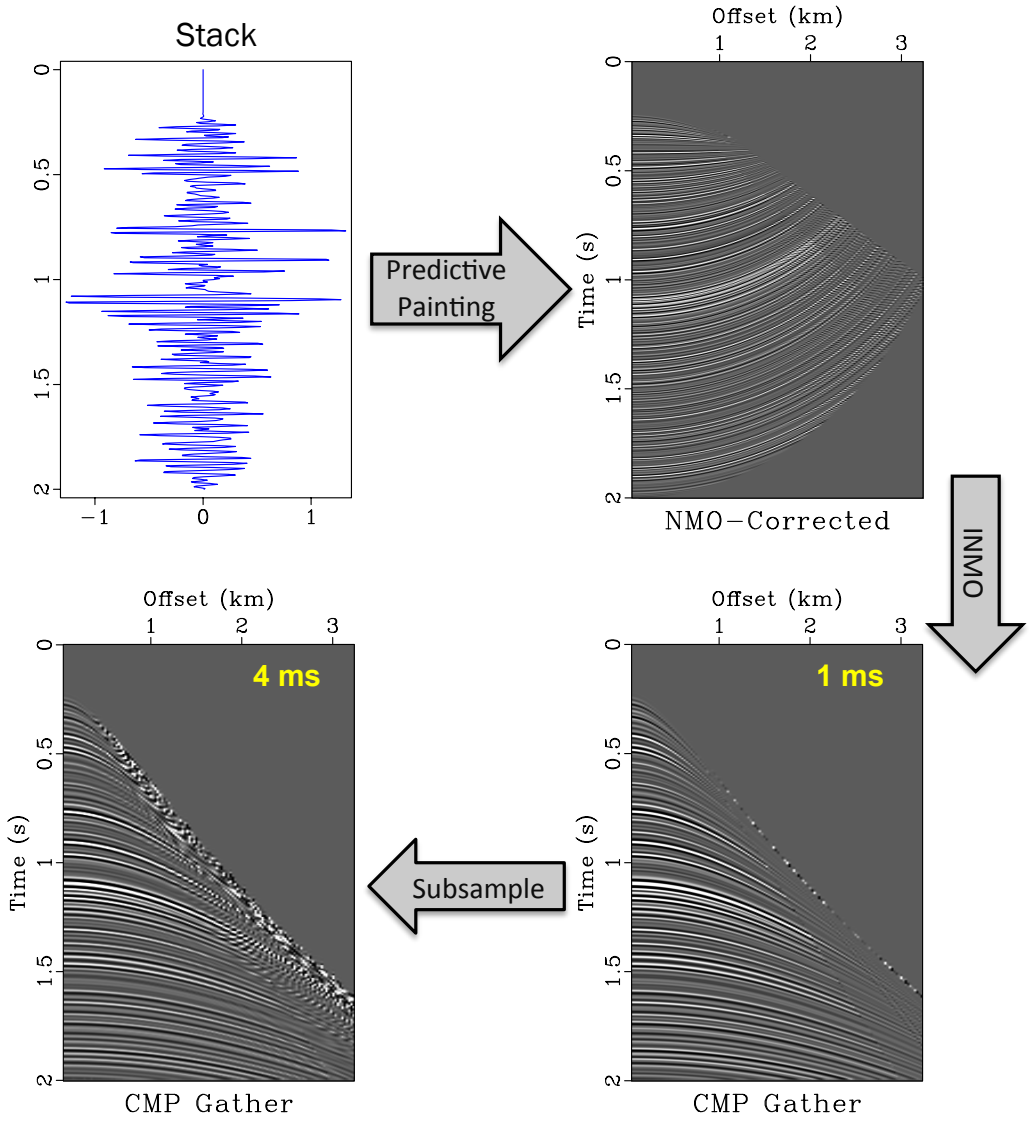

Figure 4.2: Schematic example of the forward operator in shaping regularization going from the model space (stack) to the data space (CMP gather). The forward operator consisted of three steps: predictive painting to spread information using a known dip field, inverse NMO correction with a constant velocity, and subsample in time to a sparser grid (1 ms to 4 ms). ch04-shseislet/ pwForward1

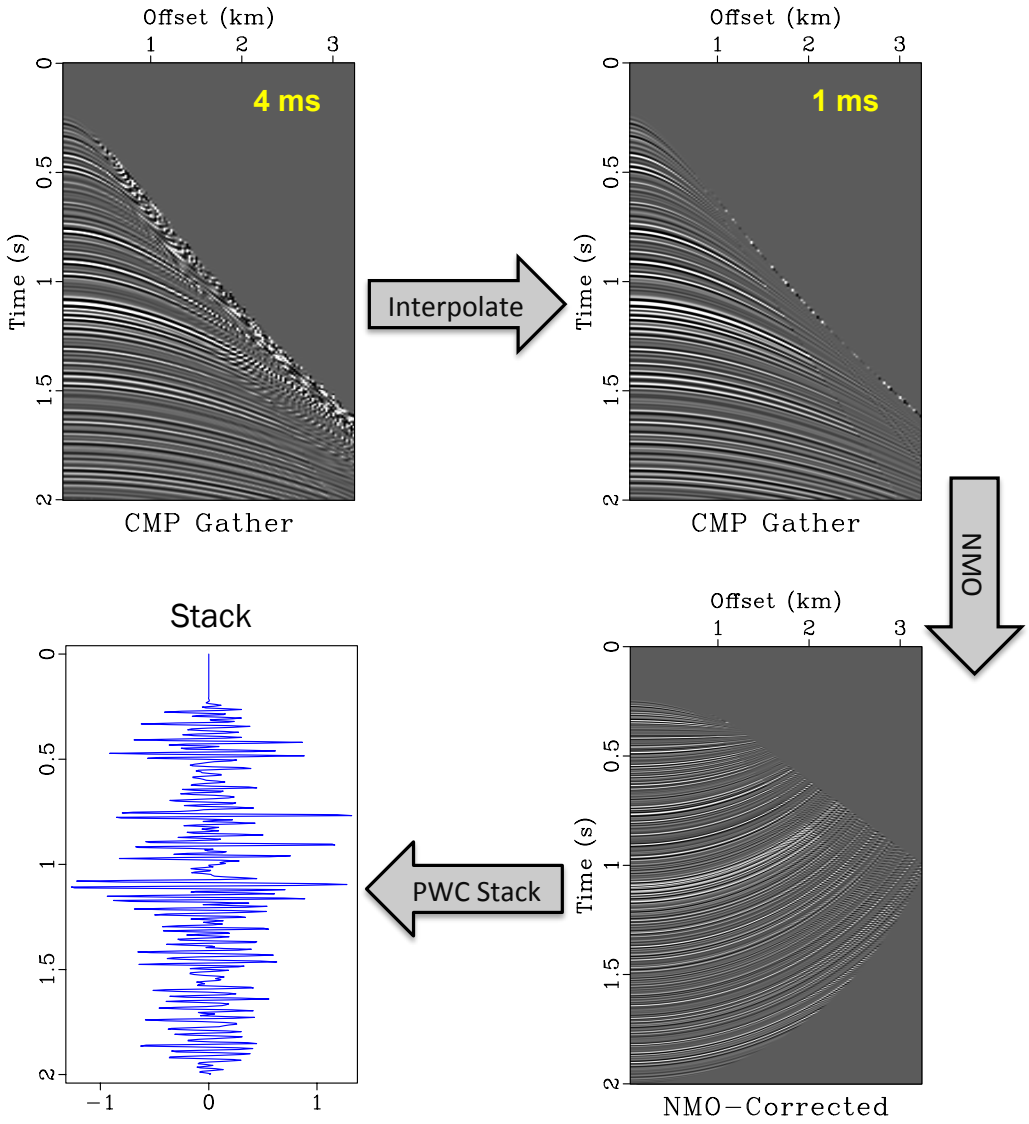

Figure 4.3: Schematic example of the backward operator in shaping regularization going from the data space (CMP gather) to the model space (stack). The backward operator is comprised of three main steps: spline interpolation in time to a denser grid (4 ms to 1 ms), NMO correction using a constant velocity and stack in a recursive fashion using local slopes. ch04-shseislet/ pwBackward1

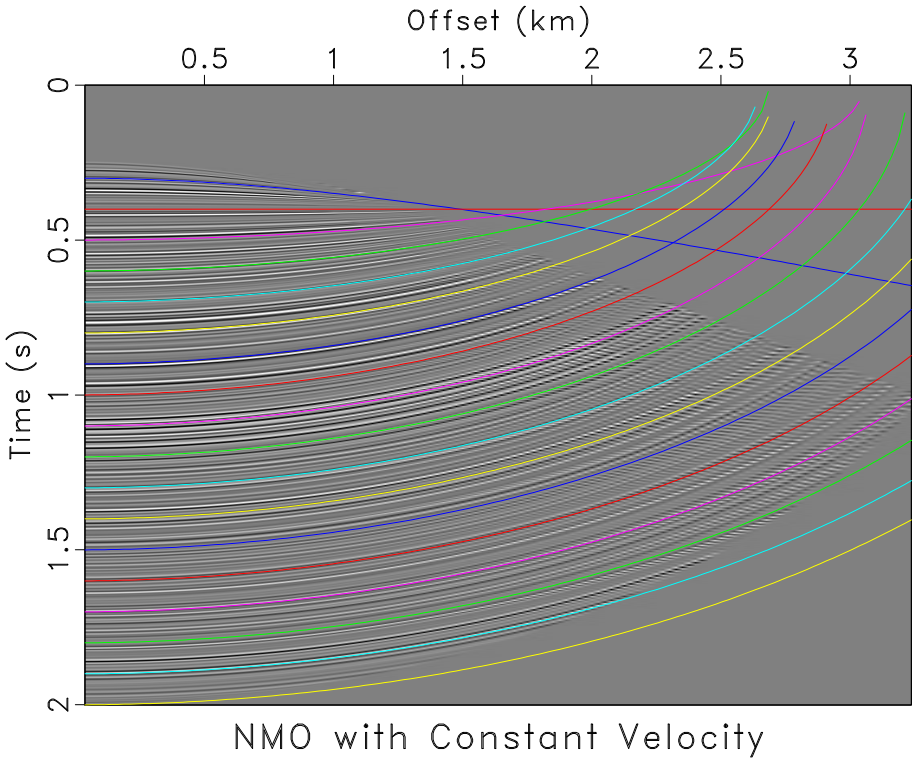

Figure 4.4: Constant velocity NMO correction using minimum velocity. Estimated moveout (equation 4.1) is overlain to demonstrate how the crossing events now occur outside of the data. Using this approximation as the initial model for PWD, I am able to compute a more accurate dip field. ch04-shseislet/seislet nmo01

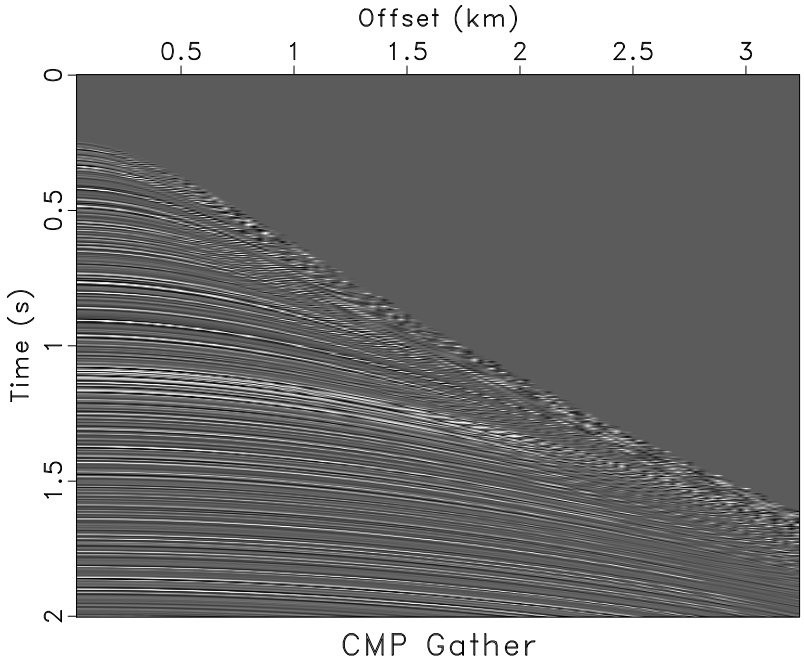

(a)

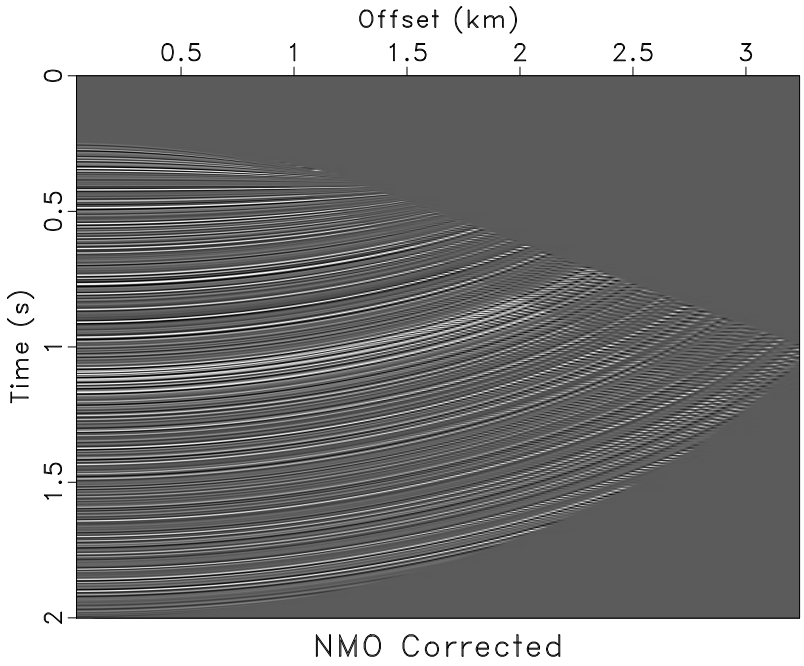

(b)

Figure 4.5: (a) Synthetic CMP gather with a 4-ms sampling interval and (b) constant velocity NMO-corrected gather to separate crossing events at far offsets. ch04-shseislet/seislet cmp2,nmo0

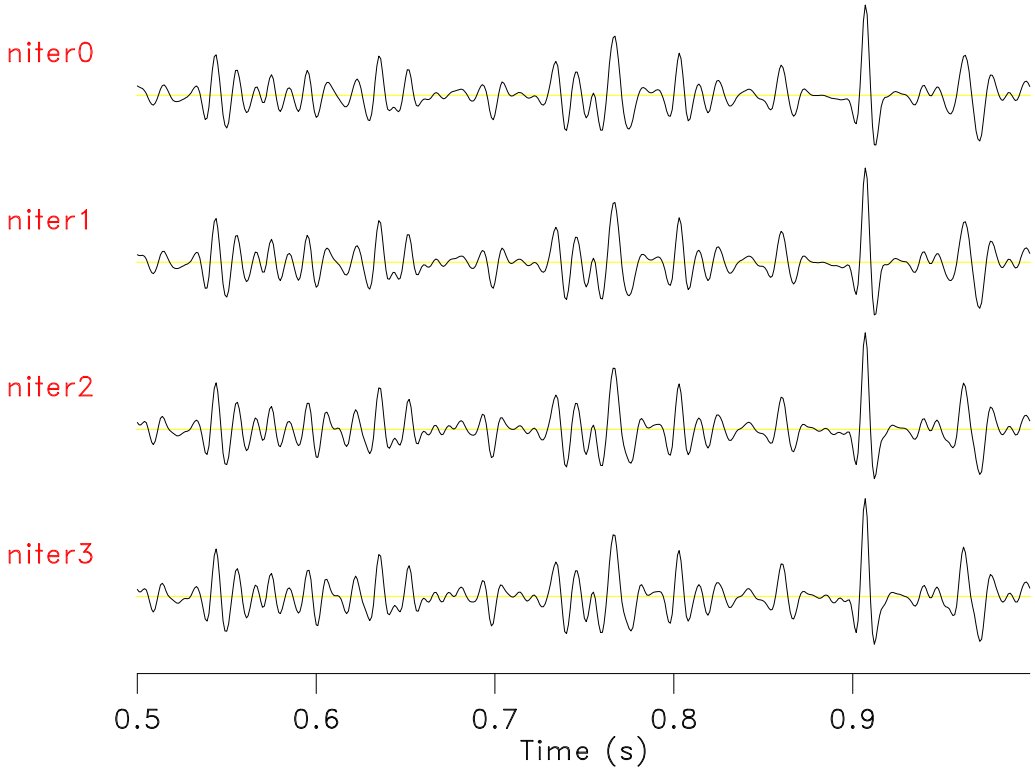

Figure 4.6: Estimated PWC stack as function of iteration using shaping regularization. Top: iteration 0 is the initial model and bottom: iteration 3 is the estimation result where convergence occurs. ch04-shseislet/seislet mod1

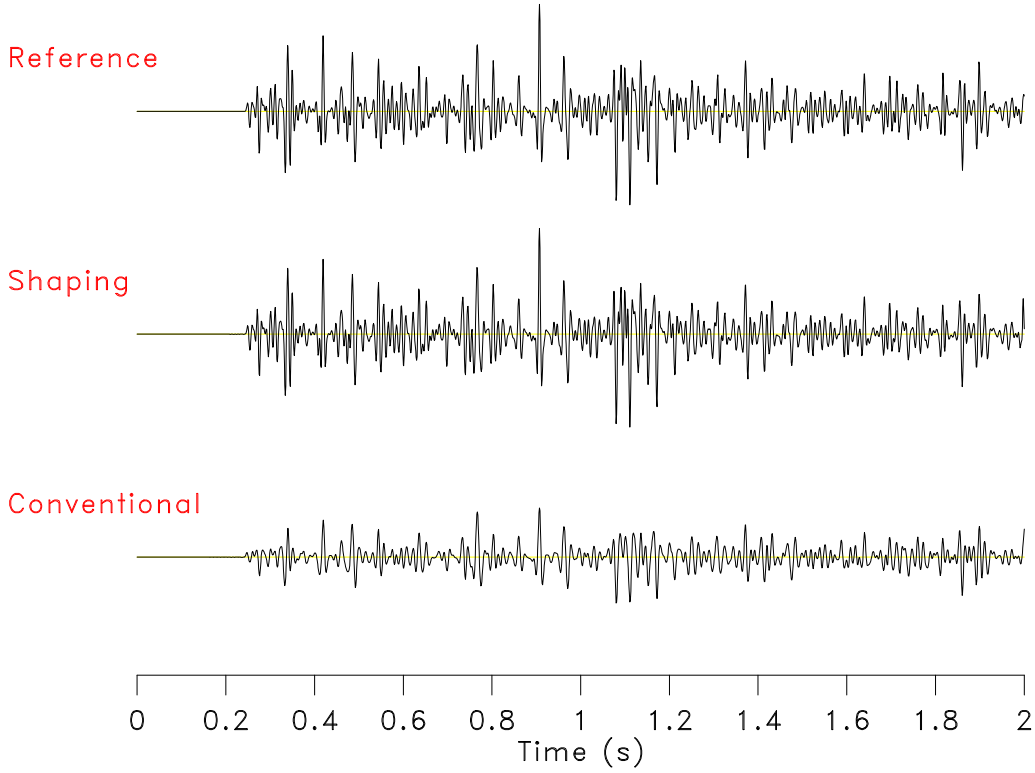

Figure 4.7: Estimated PWC stack compared with the conventional stack and the reference trace. ch04-shseislet/seislet pwmod3

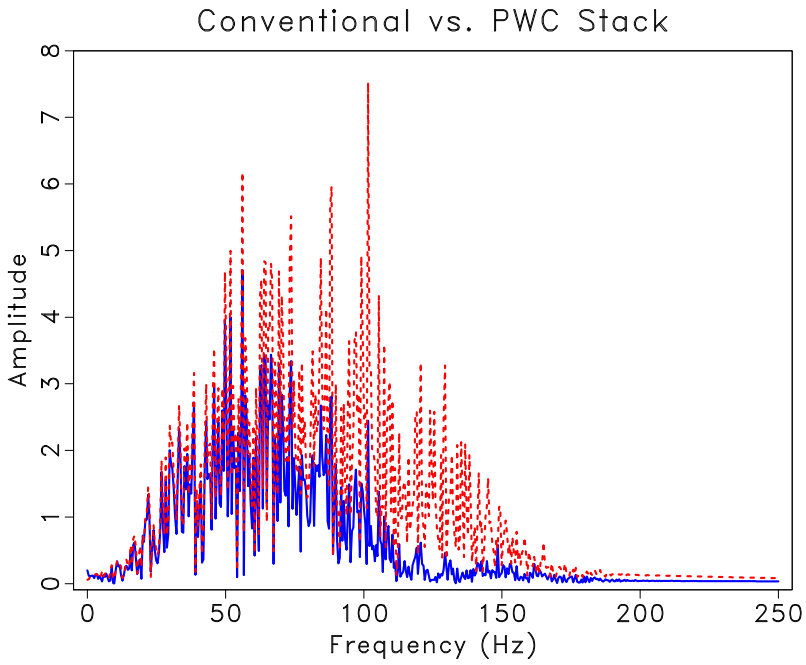

(a)

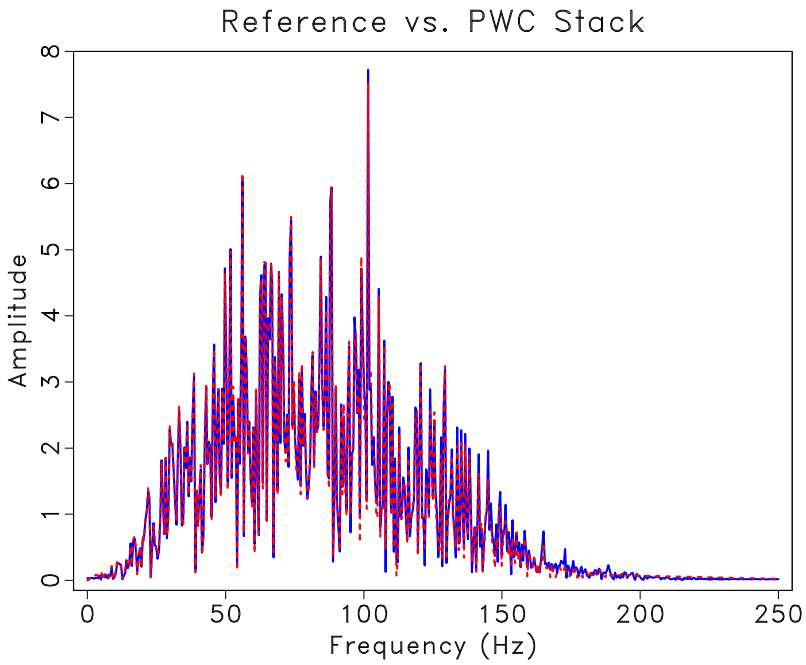

(b)

Figure 4.8: Spectral comparison of the PWC stack (dashed red) with (a) conventional NMO and stack (blue) and (b) the reference trace (blue) with a 1-ms sampling interval. ch04-shseislet/seislet spec5,spec6

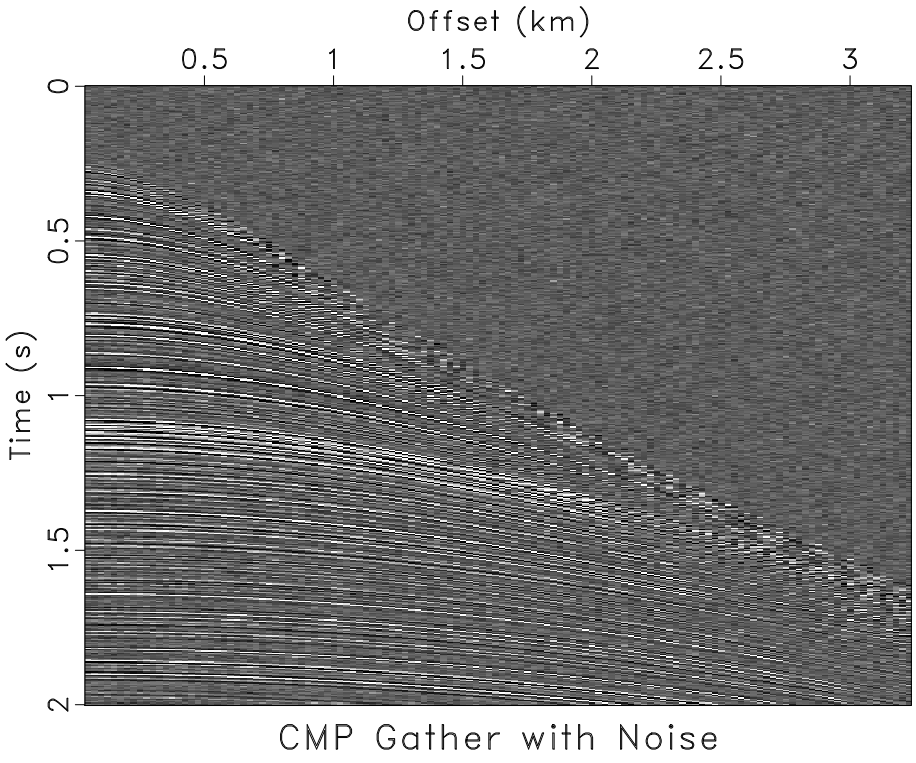

Figure 4.9: Synthetic CMP gather with random noise, which is used as the input data for PWC stack and conventional NMO and stack. ch04-shseislet/seislet cmpnoise

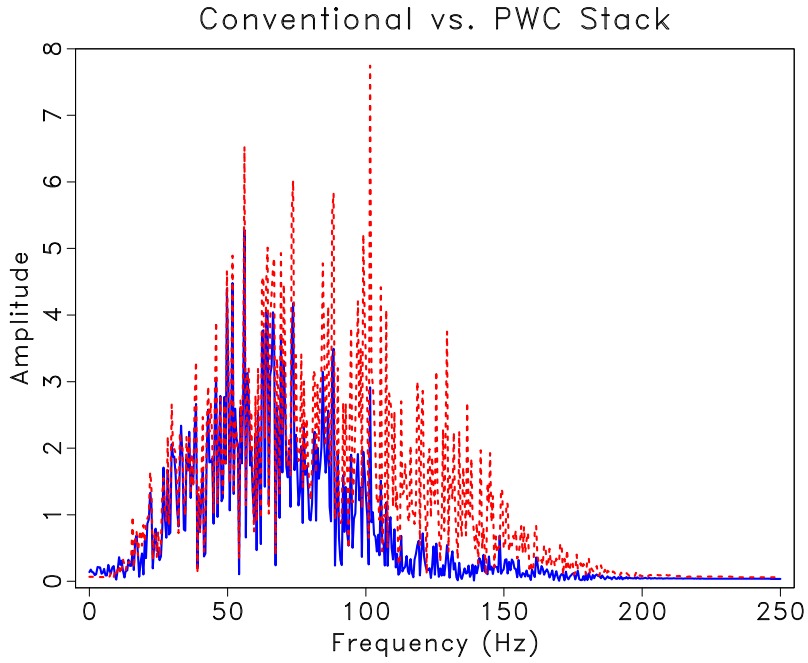

(a)

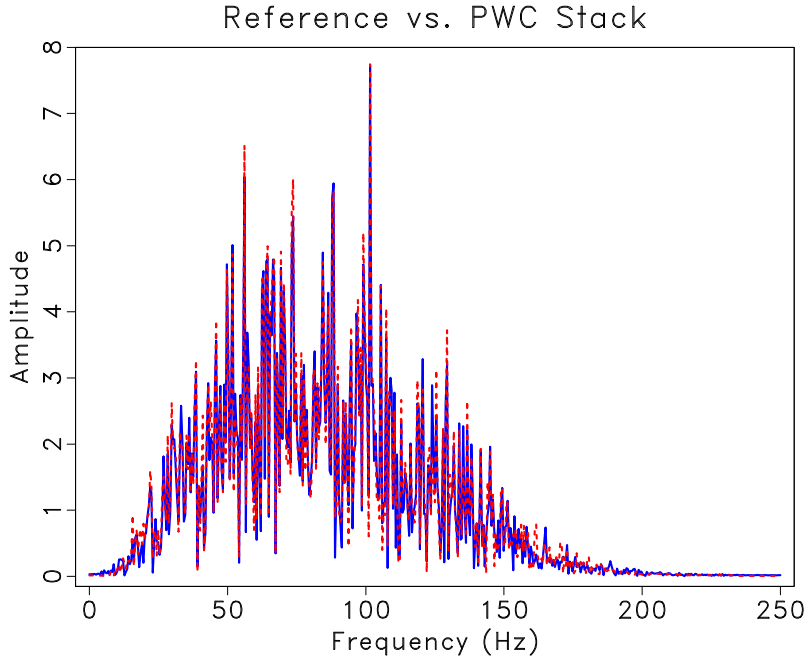

(b)

Figure 4.10: Resulting spectral comparisons of stacks with random noise applied to input data. Spectrum of the PWC stack (dashed red) vs. (a) spectrum of conventional stack (blue) and (b) spectrum of reference trace (blue) with 1-ms sampling interval.
ch04-shseislet/seislet specnoise2,specnoise1

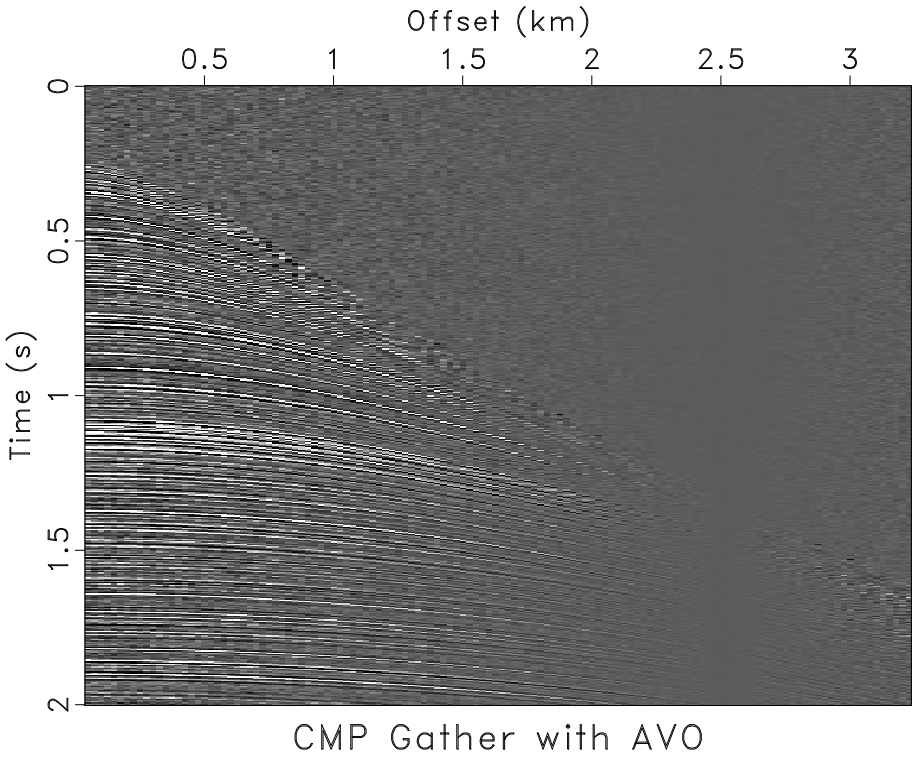

Figure 4.11: Synthetic CMP gather with random noise and artificial AVO effects, where amplitude decreases with offset. ch04-shseislet/seislet cmpavo

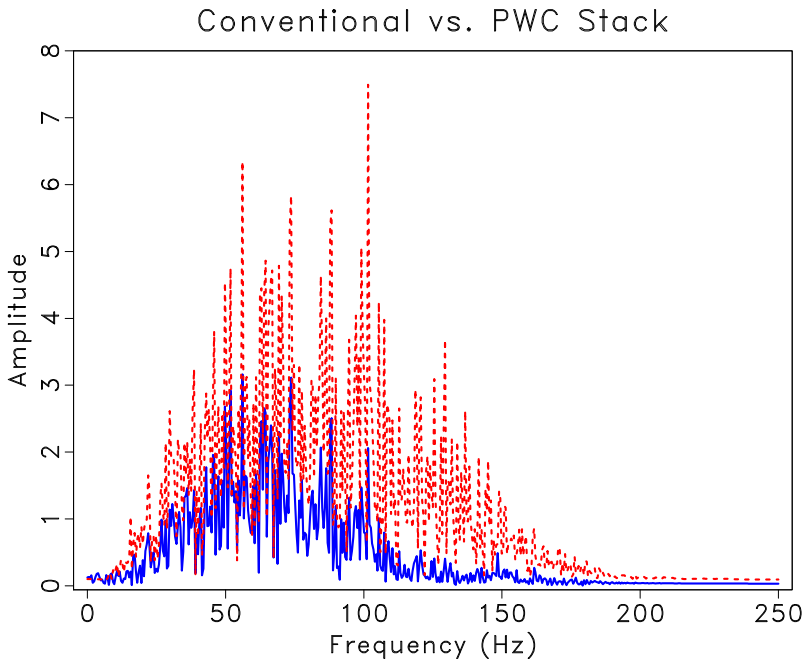

(a)

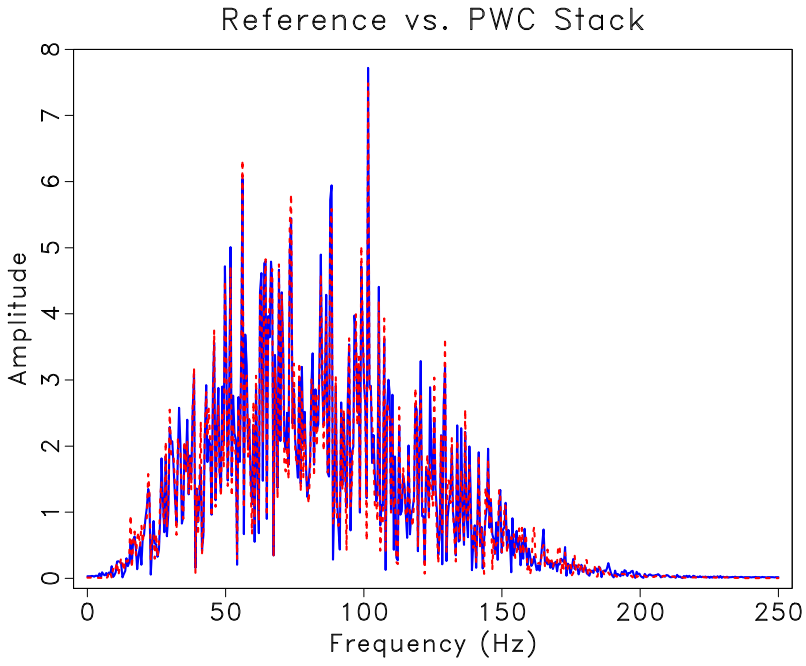

(b)

Figure 4.12: Spectral comparison of resulting stacks with random noise and artificial AVO effects applied to input data. Spectrum of the PWC stack (dashed red) with (a) conventional NMO and stack (blue) and (b) the reference trace (blue) with a 1-ms sampling interval. ch04-shseislet/seislet specavo2,specavo1

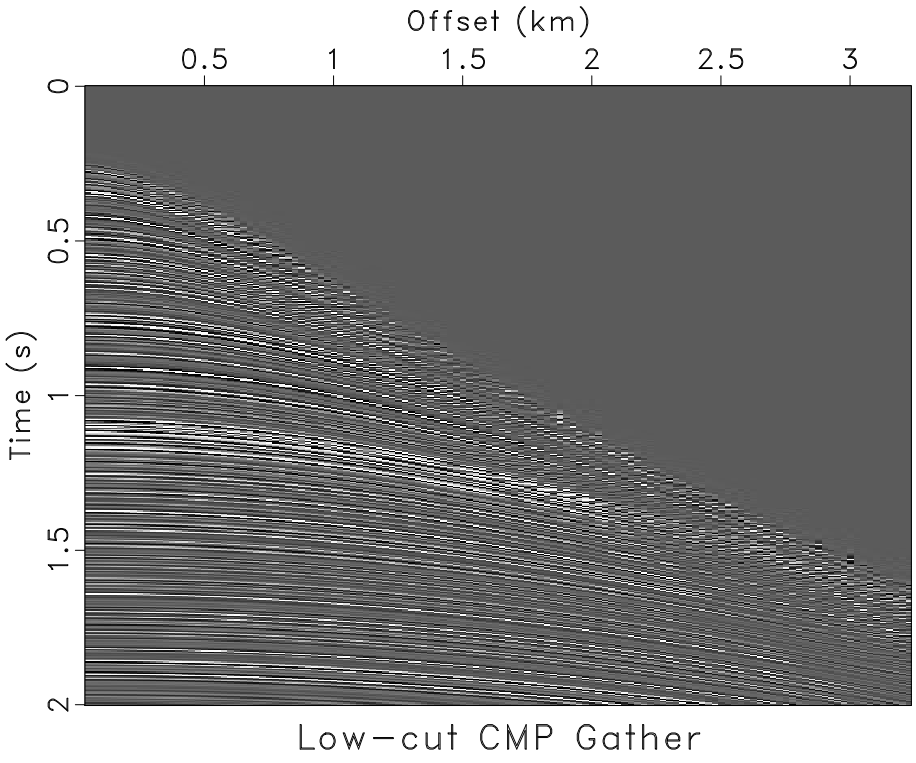

Figure 4.13: Synthetic CMP gather with a low-cut filter applied, cutting out all frequencies below 25 Hz. ch04-shseislet/seislet cmplow

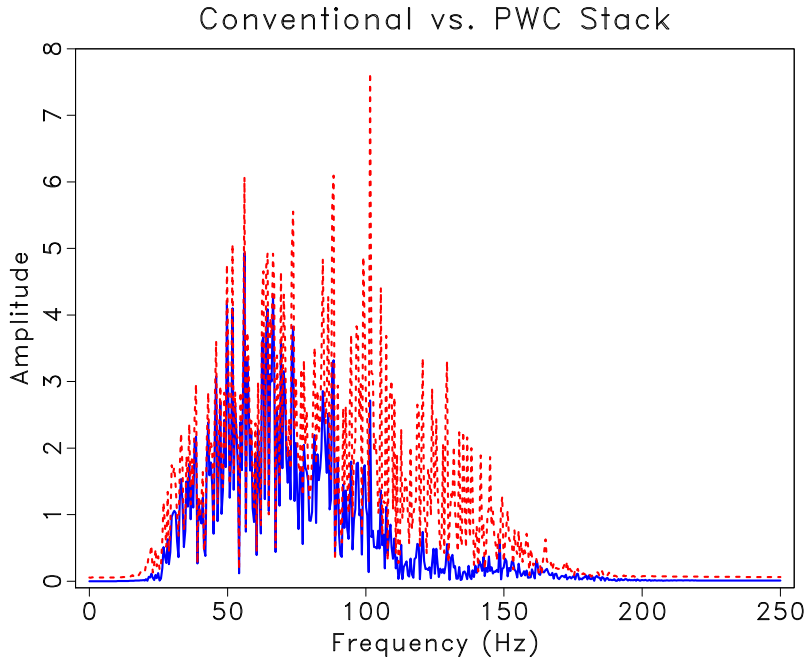

(a)

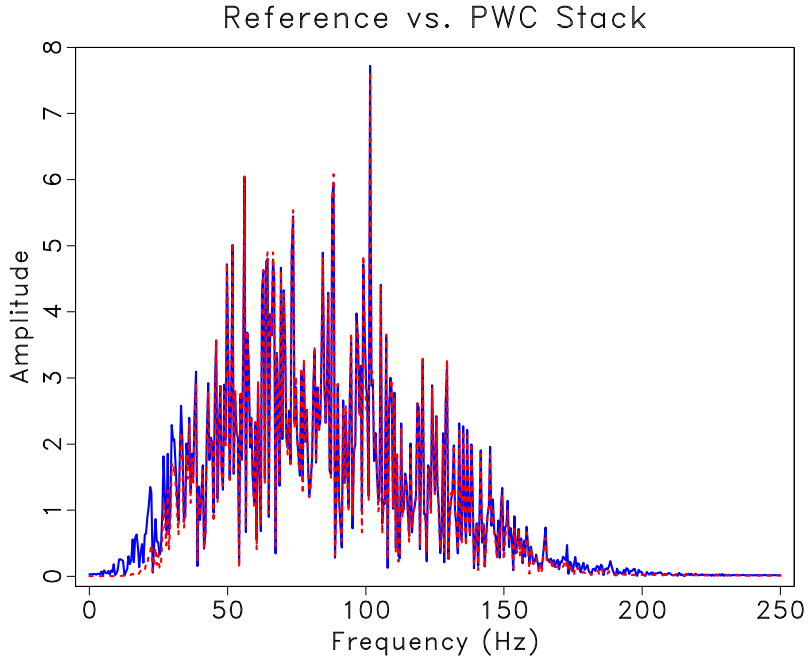

(b)

Figure 4.14: Spectral comparison of resulting stacks with a low-cut filter applied to input data. Spectrum of the PWC stack (dashed red) vs. (a) conventional NMO and stack (blue) and (b) the reference trace (blue) with a 1-ms sampling interval. ch04-shseislet/seislet speclow2,speclow1

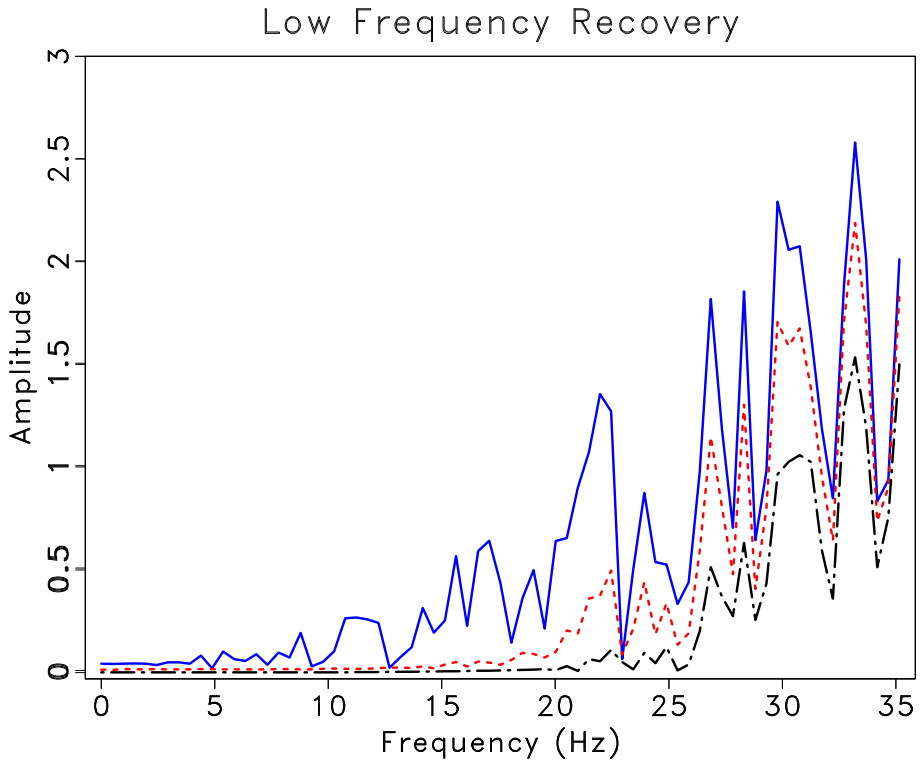

Figure 4.15: Spectral comparison of the low frequencies recovered. PWC stack (dashed red) recovers lower frequencies in comparison with the conventional stack (dot-dash black) and is consistent with the reference trace (blue). ch04-shseislet/seislet speclow3

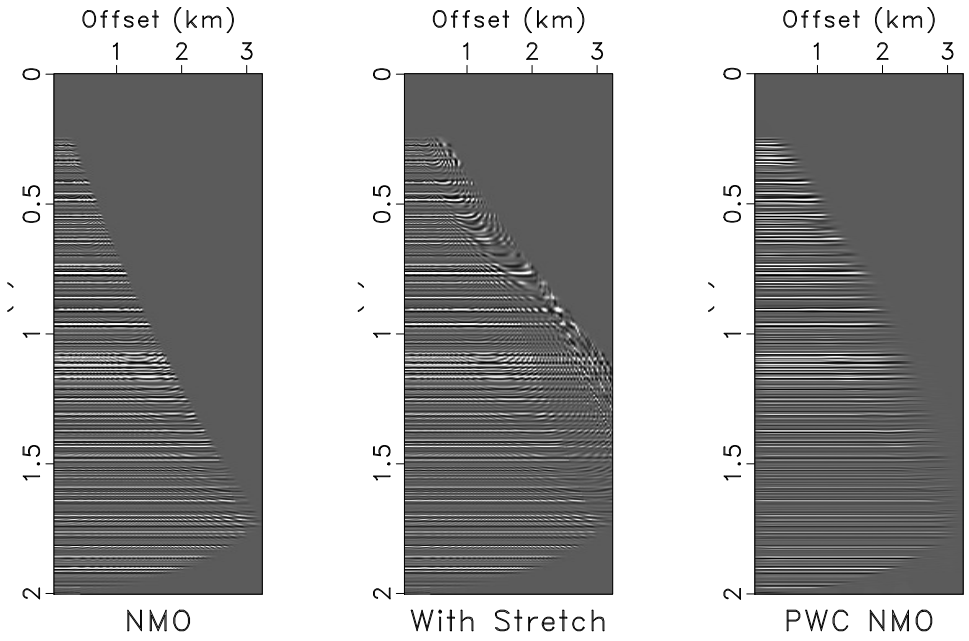

(a) (b) (c)

Figure 4.16: (a) Conventional NMO correction, (b) NMO correction without stretch muting and (c) effective NMO correction using PWC stack. ch04-shseislet/seislet nmo3,nmo2,nsnmo

Chapter 5

Field seismic data examples

In this chapter, I apply the shaping NMO stack from chapter 3 and PWC stack from chapter 4 to a 2-D field dataset from the North Sea and the 2-D Viking Graben dataset. The resulting stacked sections show noticeable resolution improvements compared with that of conventional NMO and stack.

2-D NORTH SEA DATA

The first field dataset I tested is from the North Sea and was used previously by (Fomel, 2006; Fomel and Liu, 2010). This 2-D dataset was recorded over a complex salt dome region, displayed in Figure 5.6. I apply both methods to this dataset and compare the results to conventional NMO stack. This dataset has 1,000 CMP locations and 800 samples per trace with a sampling interval of 4 ms. I apply conventional NMO and stack to the 4-ms data to use as a reference for testing the accuracy of the stacking approaches and subsample the data to 8 ms to provide the input data for shaping NMO stack, PWC stack and conventional NMO stack. The shaping operator used is a bandpass filter ranging from 2 Hz to 100 Hz for shaping NMO stack and 3 Hz to 110 Hz for PWC stack. The parameters were selected based on the frequency content of the data. The estimation result using shaping regularization is sensitive to the defined bandpass filter. Upper frequency bounds that are too high may lead to spurious high frequencies in the stack. Figure 5.1 demonstrates the effect of incorrect

bandpass filter boundaries. In this figure, the spectrum of shaping NMO stack using a bandpass filter ranging from 2 Hz to 90 Hz (dashed red) is compared to shaping NMO stack using a bandpass filter ranging from 2 Hz to 124 Hz (blue). By using an upper bound that is too large in the latter case, spurious high frequencies are introduced. Therefore, the bounds of the bandpass filter are data-dependent and must be selected based on the frequency content of the data. The convergence of shaping NMO stack required 5 iterations, while PWC stack required only 3 iterations. In Figure 5.2, the result of applying the shaping methods to one CMP gather is compared to the resulting stacks from conventional NMO and stack and the reference stack, which is NMO and stack using the densely sampled 4-ms data. The frequency content and amplitude of the PWC stack appear to be the highest of the different stacking methods. I next evaluate the spectral content recovered for each approach. I first compare the frequency content of the PWC stack to that of the shaping NMO stack, shown in Figure 5.3. The PWC stack recovers slightly higher frequencies compared to the shaping NMO stack. The spectrum of the shaping NMO stack is next compared to that of conventional NMO and stack in Figure 5.4(a) and the spectrum of the densely sampled reference stack in Figure 5.4(b). Compared to the conventional stack, the shaping NMO stack recovers extra bandwidth with higher frequencies present, which range to 80 Hz. The accuracy of the recovered high frequencies is supported by the spectral comparison of the shaping NMO stack and the reference stack. I next analyze the ability of PWC stack to accurately recover higher frequencies, shown in Figure 5.5. The PWC stack recovers higher frequency content compared to the conventional stack and also lower frequency content as demonstrated in Figure 5.5(a). Compared to the dense stack (Figure 5.5(b)), PWC stack recovers slightly higher frequencies but is overall consistent with the spectral content of the dense stack. The resulting stacked

sections using the 8-ms data as the input are displayed in Figures 5.6, 5.7, and 5.8. For shallow reflectors, higher frequencies exist using shaping NMO stack and PWC stack in comparison with conventional NMO stack, which suggests that the effects of "NMO stretch" are reduced. This is seen clearly in Figure 5.9, which is a zoomed in section of a shallow region of the stacked sections. The PWC stacking approach recovers the most information out of the three approaches based on the thin layers that are resolved in Figure 5.9. I zoom into a different portion of the dataset in Figure 5.10, which is near the top of the salt diapir. This figure demonstrates that both algorithms have the ability to resolve thin layers in a complex geologic medium. Throughout the entire section, PWC stack and shaping NMO stack recover significantly higher frequencies compared to the conventional stack. Thin layers that are unclear in the conventional stacked section become clearly resolved and continuous in the PWC and shaping NMO stacked sections. Overall, events become more continuous and coherent throughout the section using PWC stack, and overall resolution is noticeably improved.

VIKING GRABEN DATA

The next dataset I tested the stacking approaches on is the 2-D Mobil AVO Viking Graben Line 12, also from the North Sea (Keys and Foster, 1998). The dataset used was preprocessed, and most of the multiple reflections were attenuated. However, residual multiple energy still remains in the dataset. This dataset contains 2,142 CMP locations and 1,001 samples per trace with a sampling interval of 4 ms. I subsample the data to 8 ms, which was the input for PWC stack, shaping NMO stack and conventional NMO stack. I apply conventional NMO and stack to the 4-ms data, which allowed us to have a densely-sampled reference stack in order to evaluate the

accuracy of the shaping stack methods in recovering a broader frequency band. The shaping operator used is a bandpass filter ranging from 3 Hz to 90 Hz for shaping NMO stack and 2 Hz to 90 Hz for PWC stack. The convergence of shaping NMO stack required 6 iterations, while PWC stack required only 4 iterations. The result of applying each method to one CMP location is shown in Figure 5.11. The conventional 8-ms stack appears to contain the lowest resolution, while the shaping stacks contain higher frequencies that are similar to the dense 4-ms stack. I next analyzed the frequency content recovered by comparing the spectral bands of each stack. I first compare the spectrum of the PWC stack and shaping NMO stack in Figure 5.12. Overall, the frequency content recovered using both methods is similar, however, the shaping NMO stack recovers slightly lower frequencies than the PWC stack. The spectrum of the shaping NMO stack is compared to that of the conventional stack in Figure 5.13(a) and the spectrum of the densely-sampled reference stack in Figure 5.13(b). The shaping NMO stack recovers significantly higher frequencies compared to the conventional stack that are consistent with the dense stack. The shaping NMO stack also recovers slightly lower frequencies than the conventional stack. I next examine the frequency content of the PWC stack in comparison to the conventional stack in Figure 5.14(a) and the dense stack in Figure 5.14(b). The PWC stack is able to restore frequencies ranging to 80 Hz, while the conventional stack is limited to approximately 60 Hz. Compared to the dense stack, the frequencies recovered using the PWC stacking approach are accurate. The resulting stacked sections using the 8-ms data as the input to conventional NMO stack, shaping NMO stack, and PWC stack are displayed in Figures 5.15, 5.16, and 5.17, respectively. There are clear resolution improvements throughout the section using the shaping stack approaches in comparison with the conventional stack. Shallow sections become

more coherent and thin layers are resolved. I zoom in to a shallow portion of the stacked section, which is displayed in Figure 5.18, to clearly detect the resolution improvements. In this windowed section, there appear to be dipping beds that are truncated against a flat upper layer. By using the shaping stack approaches, these dipping layers are coherent and continuous, whereas the conventional stack appears low resolution and difficult to interpret. The flat layers above also have significant resolution improvements using the shaping stack approaches, where thinner layers are detected in comparison with the conventional stack. Overall, by implementing the stacking schemes using shaping regularization, I am able to reconstruct a higher resolution stack that is easier to interpret and not limited by the 8-ms sampling interval of the input gathers.

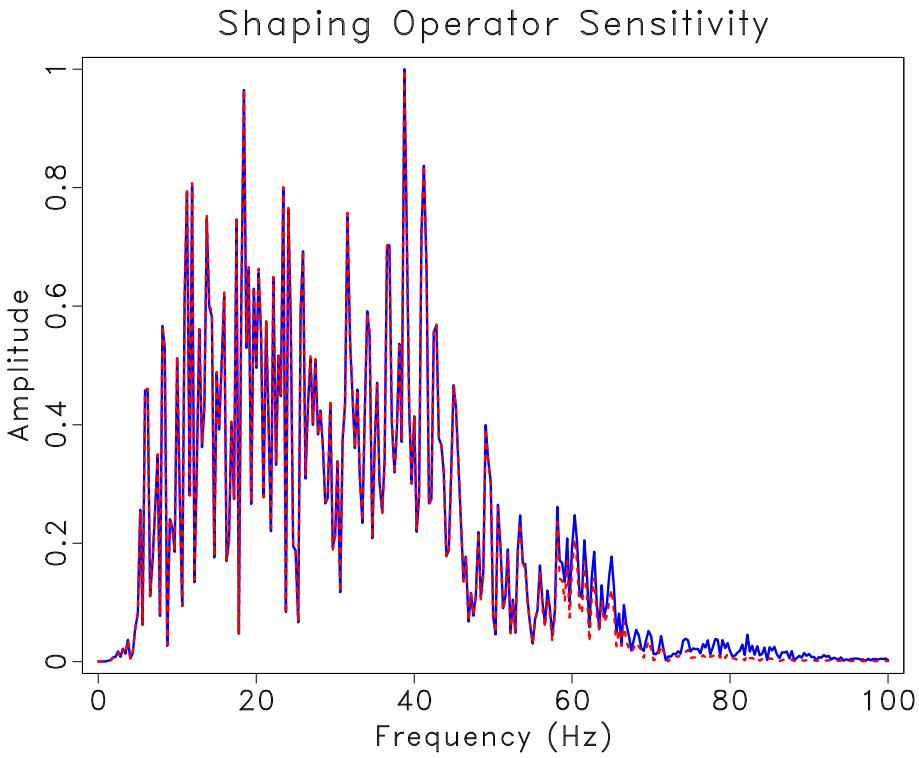

Figure 5.1: Example of sensitivity to frequency bounds using shaping regularization. Spectral comparison of shaping NMO stack using a bandpass filter ranging from 2 Hz to 90 Hz (dashed red) versus a bandpass filter ranging from 2 Hz to 124 Hz (blue). By using an upper bound that is too large, spurious high frequencies are introduced. ch05-elf/elf spec8

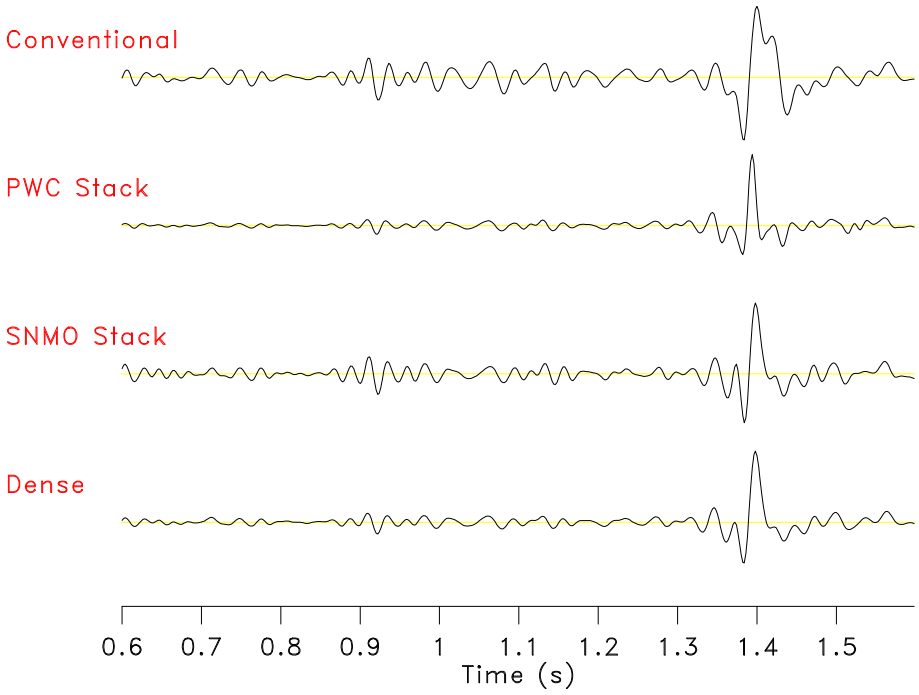

Figure 5.2: Stacked result for one CMP gather. From top to bottom: 8-ms conventional stack, PWC stack, shaping NMO stack, and dense 4-ms conventional stack ch05-elf/elf mod

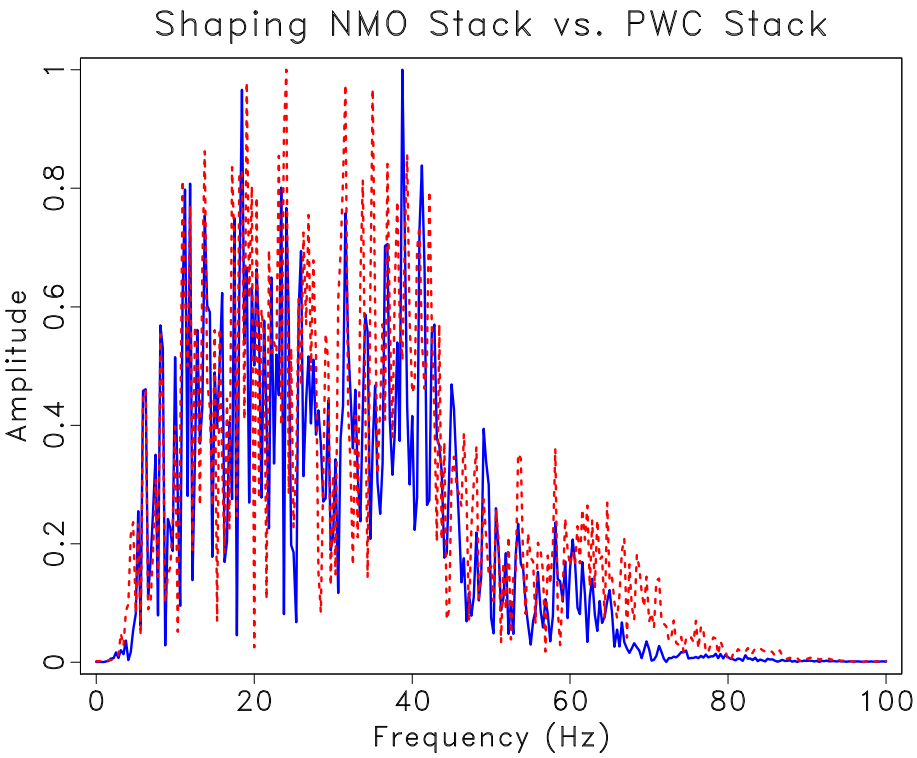

Figure 5.3: Spectral comparison of the shaping NMO stack (blue) compared to the PWC stack (dashed red). The PWC stack recovers slighly higher frequencies than the shaping NMO stack. ch05-elf/elf shpwspec

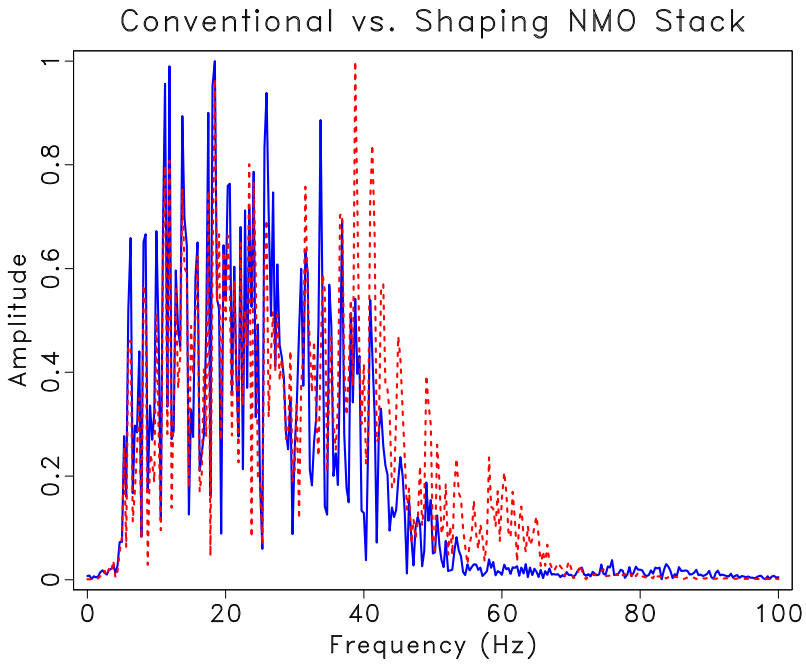

(a)

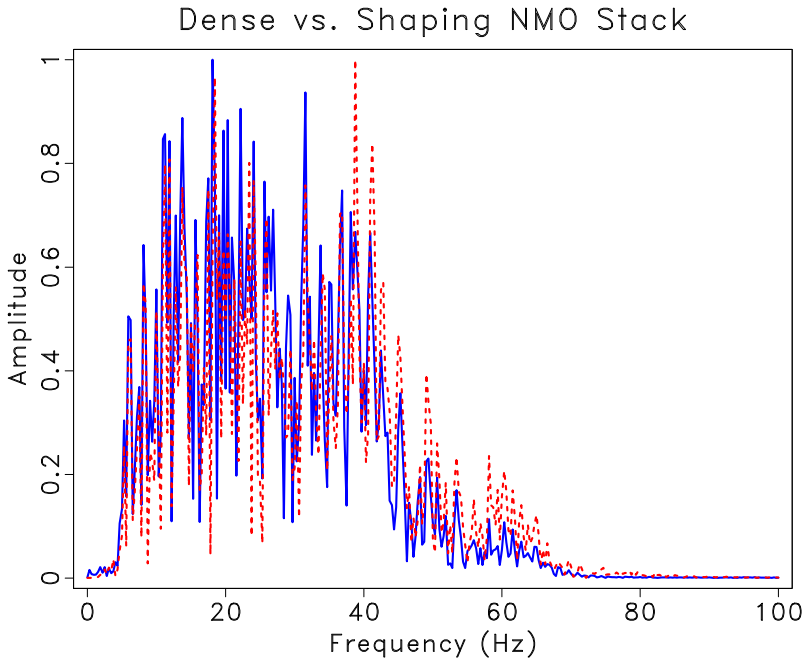

(b)

Figure 5.4: Spectrum of the shaping NMO stack (dashed red) using the subsampled 8-ms data versus (a) conventional stack (blue) using the subsampled 8-ms data and (b) conventional stack (blue) using the 4-ms data. ch05-elf/elf specn0,specn1

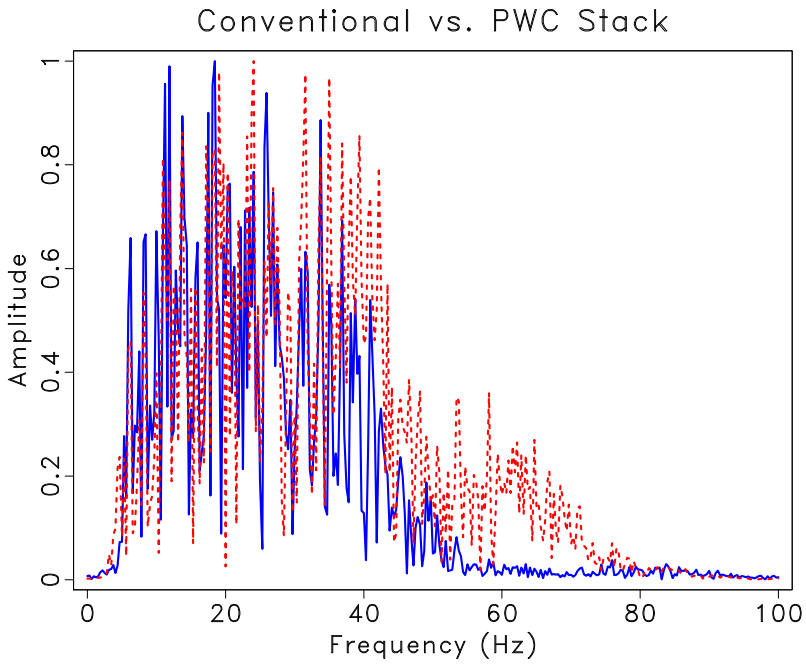

(a)

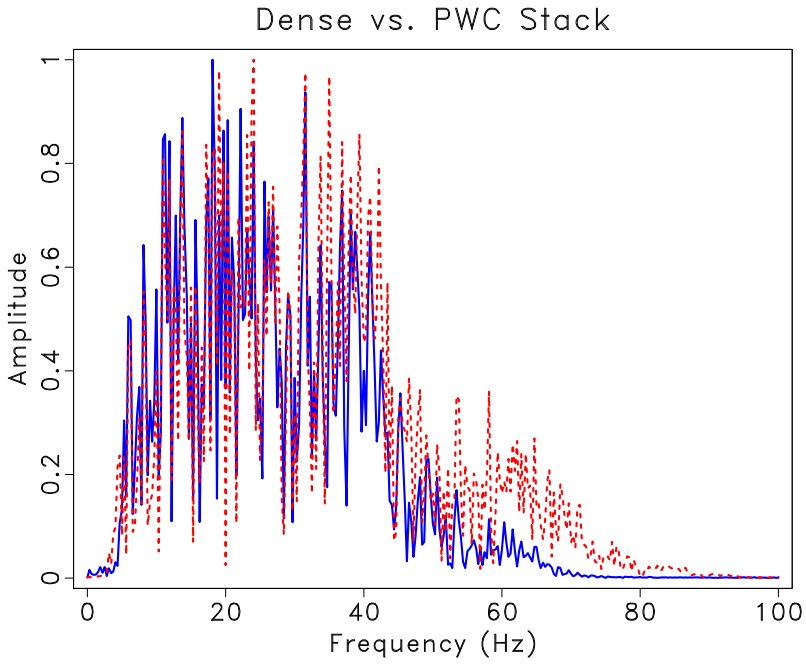

(b)

Figure 5.5: Spectrum of PWC stack (dashed red) using the subsampled 8-ms data versus (a) conventional stack (blue) using the subsampled 8-ms data and (b) conventional stack (blue) using the 4-ms data. ch05-elf/elf compspec,compspec2

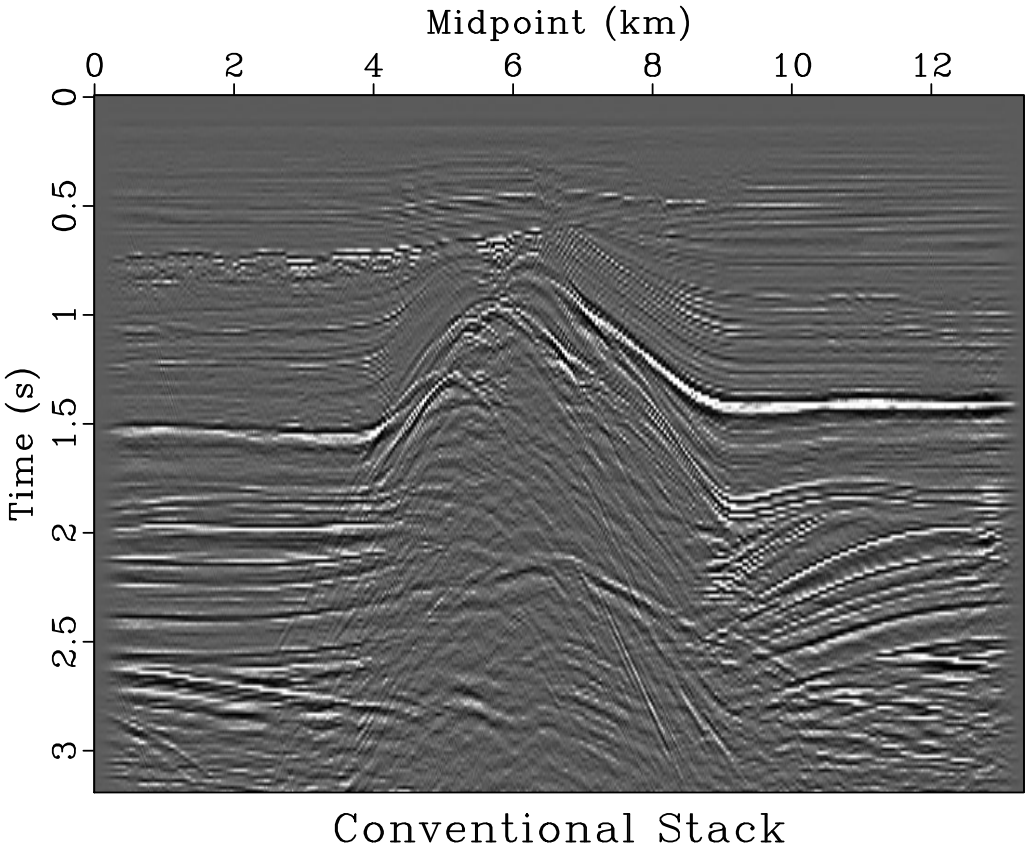

Figure 5.6: North Sea data example. NMO and stack using conventional method with 8-ms data as input. ch05-elf/elf istack

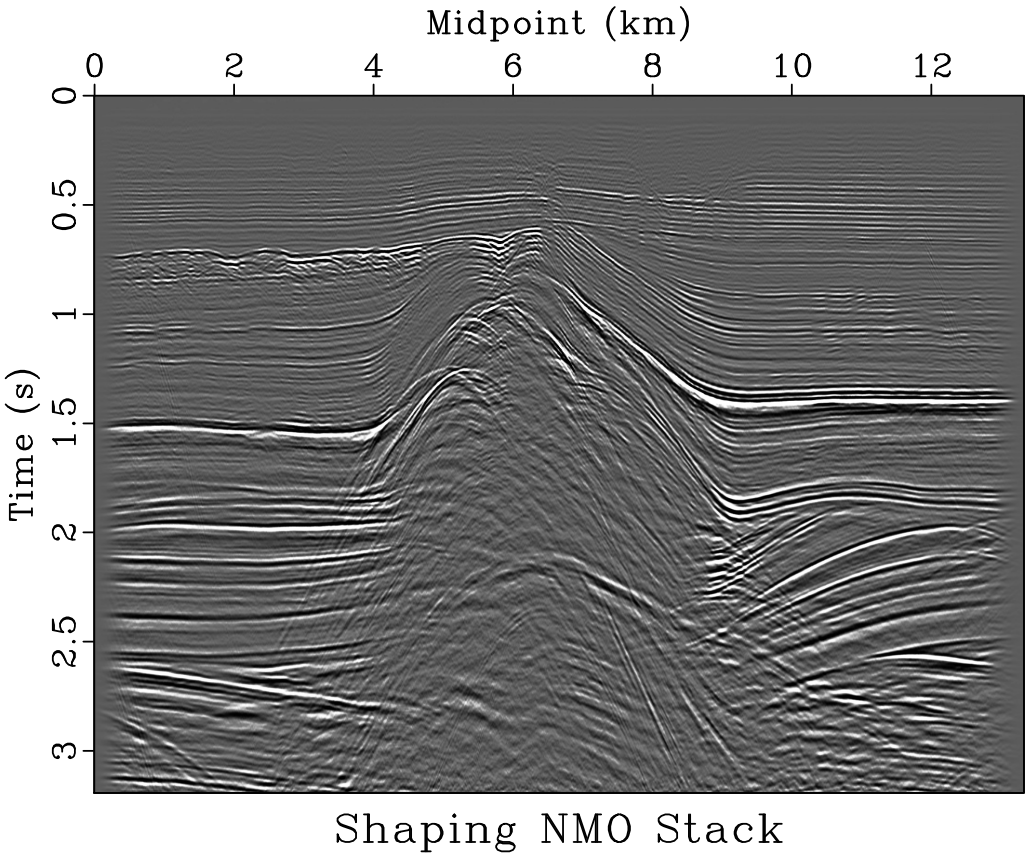

Figure 5.7: North Sea data example. NMO and stack using shaping NMO stack with 8-ms data as input. ch05-elf/elf shngmres

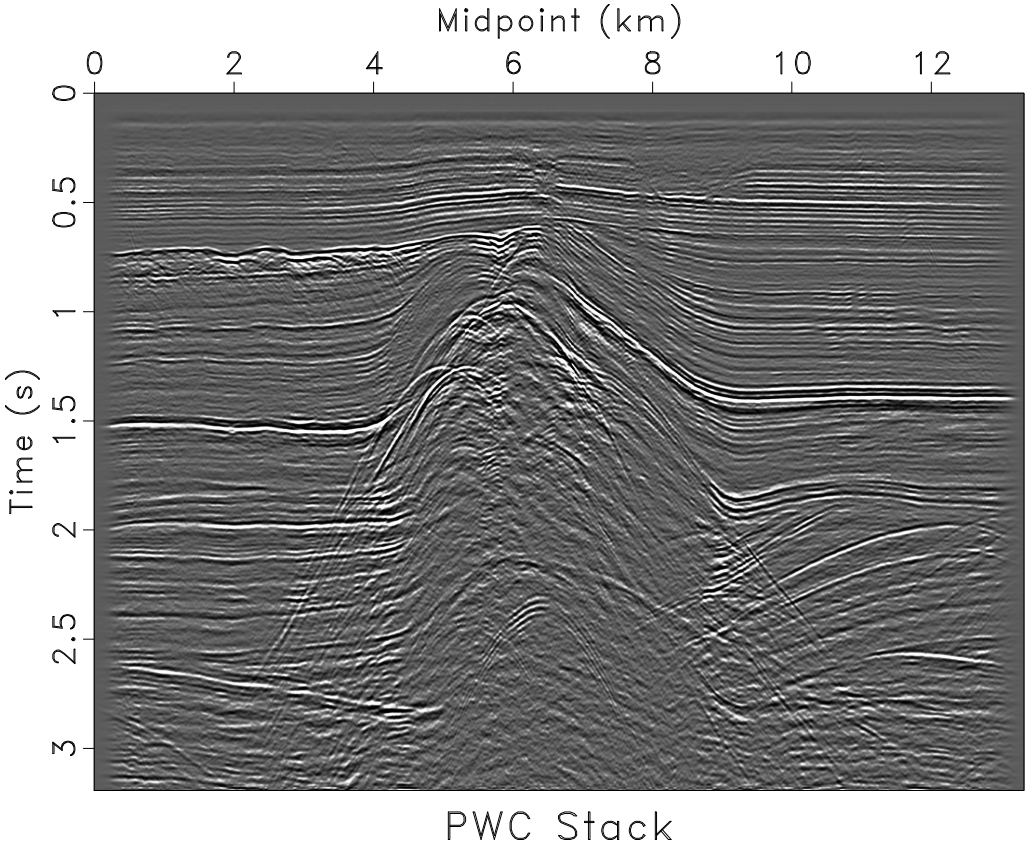

Figure 5.8: North Sea data example. NMO and stack using PWC stack with 8-ms data as input. ch05-elf/elf ungmres2

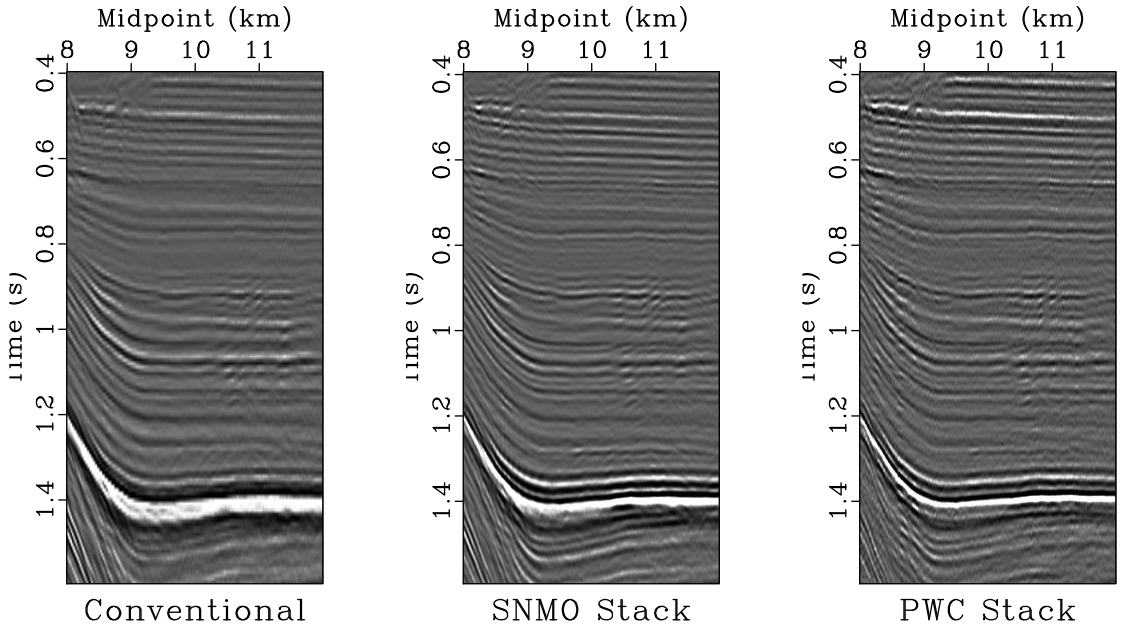

(a) (b) (c)

Figure 5.9: Zoomed in section of the North Sea data using (a) conventional NMO and stack (b) shaping NMO stack and (c) PWC stack. ch05-elf/elf wstack,shwnstack,wnstack

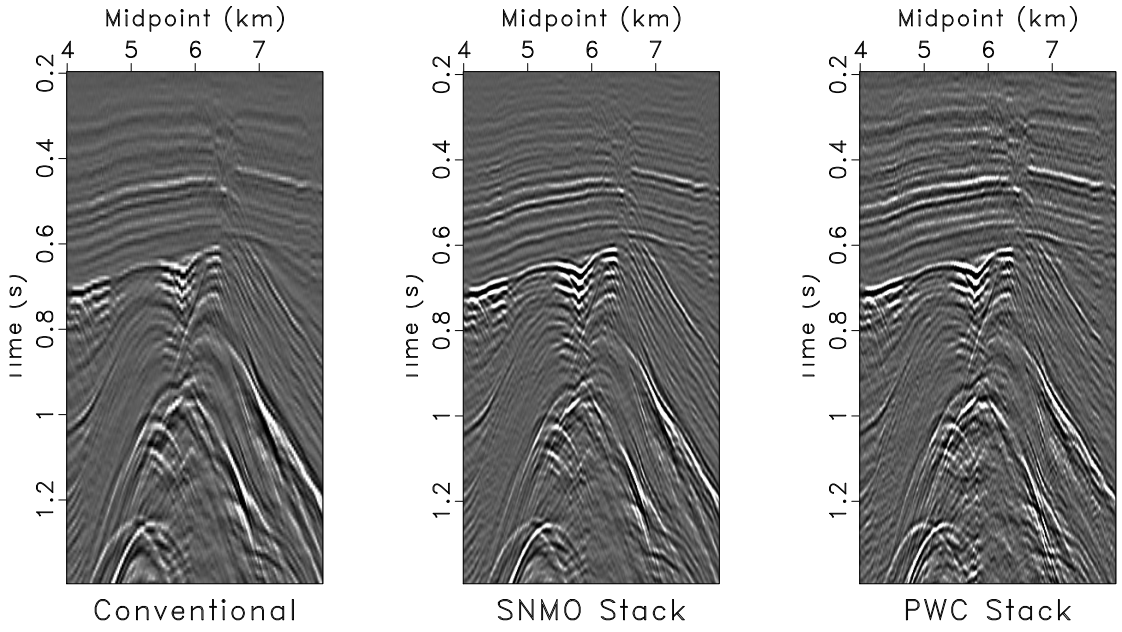

Figure 5.10: Zoomed in section of the North Sea data using (a) conventional NMO and stack (b) shaping NMO stack and (c) PWC stack. ch05-elf/elf wstack1,shwnstack1,wnstack1

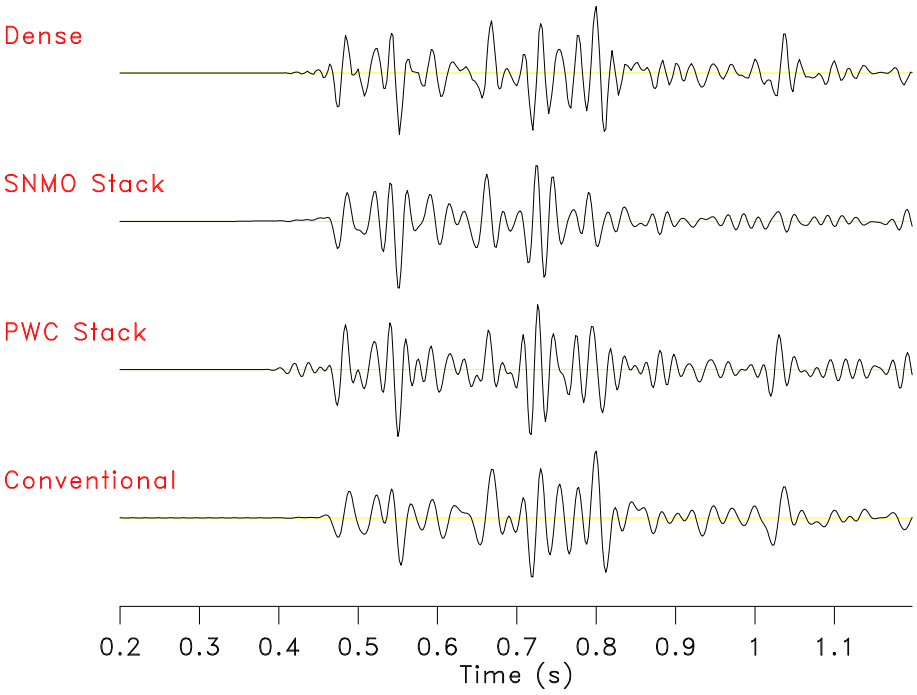

Figure 5.11: Viking Graben stacked results for one CMP gather. From top to bottom: dense 4-ms conventional stack, shaping NMO stack, PWC stack, and 8-ms conventional stack. ch05-elf/viking mod3

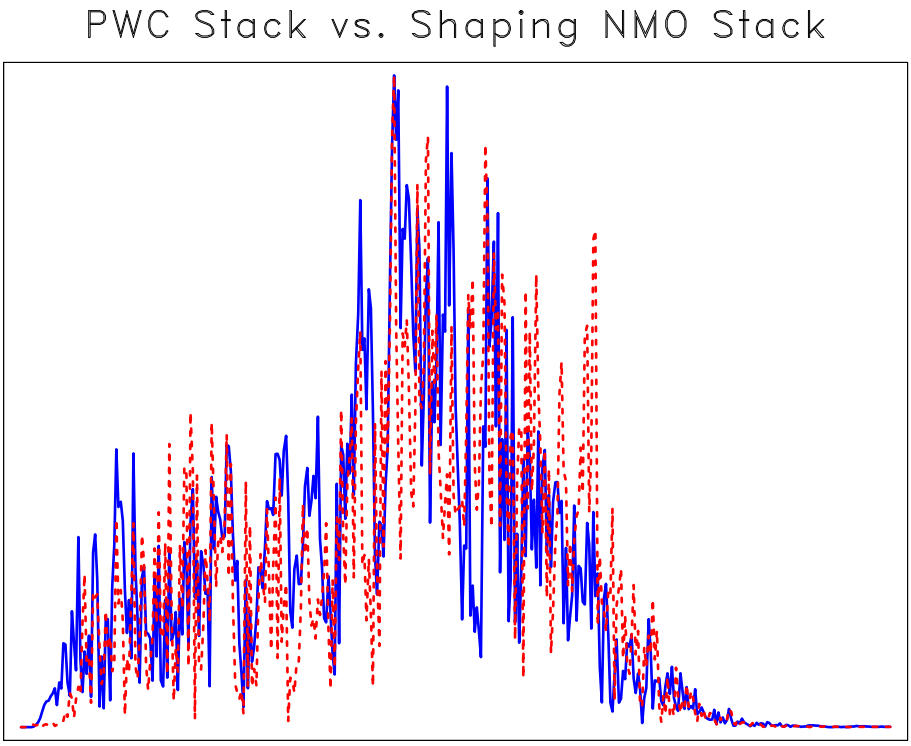

Figure 5.12: Spectral comparison of the shaping NMO stack (blue) compared to the PWC stack (dashed red). Overall, the frequency content recovered using both methods is similar, however, the shaping NMO stack recovers slightly lower frequencies than the PWC stack. ch05-elf/viking shspectest

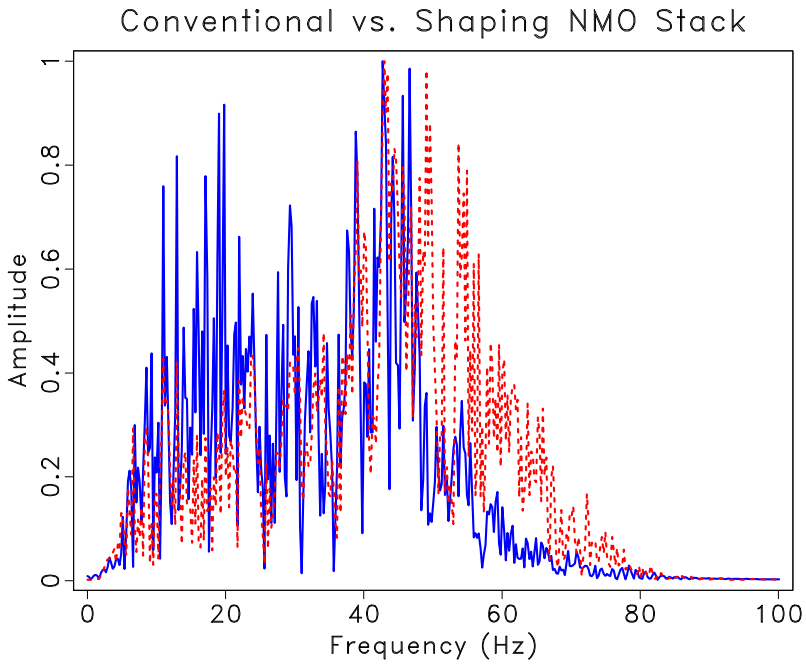

(a)

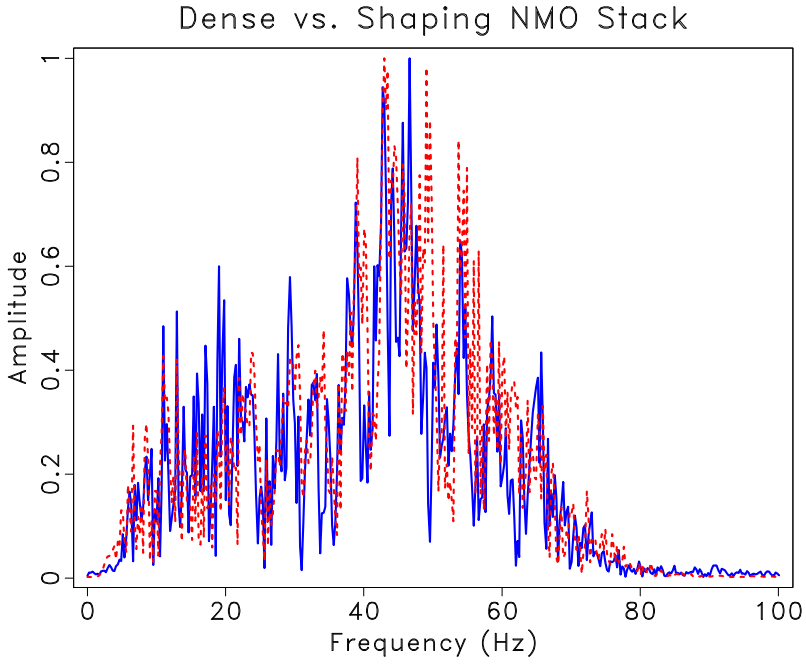

(b)

Figure 5.13: Viking Graben spectrum of the shaping NMO stack (dashed red) using the subsampled 8-ms data and 4-ms output stack versus (a) conventional stack (blue) using the subsampled 8-ms data and (b) conventional stack (blue) using the 4-ms data. ch05-elf/viking shspec1,shspec2

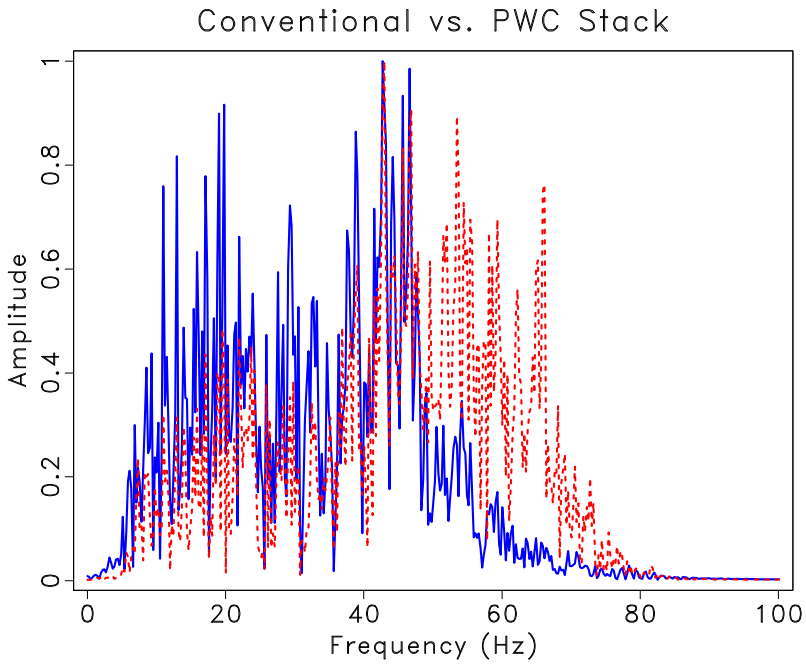

(a)

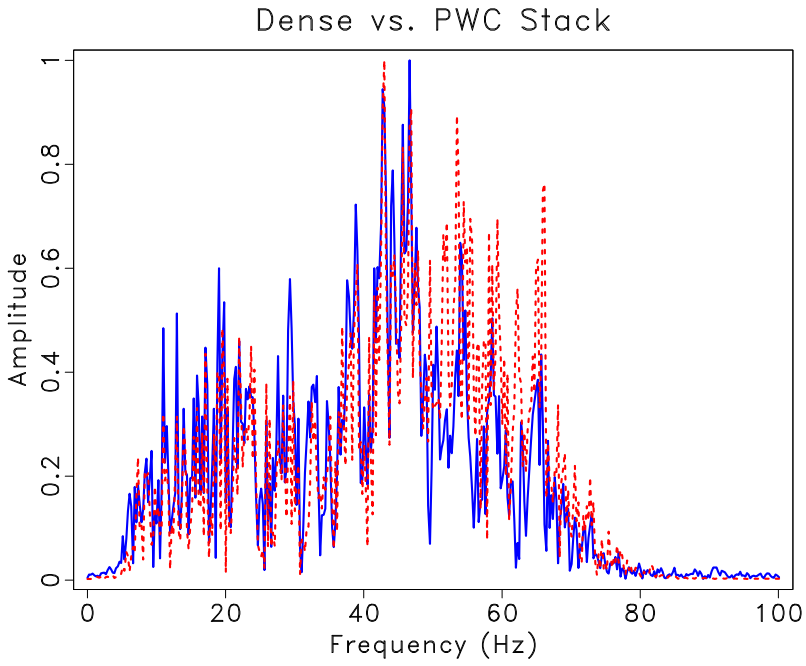

(b)

Figure 5.14: Viking Graben spectrum of PWC stack (dashed red) using the subsampled 8-ms data and 4-ms output stack versus (a) conventional stack (blue) using the subsampled 8-ms data and (b) conventional stack (blue) using the 4-ms data. ch05-elf/viking pwspec2,pwspec1

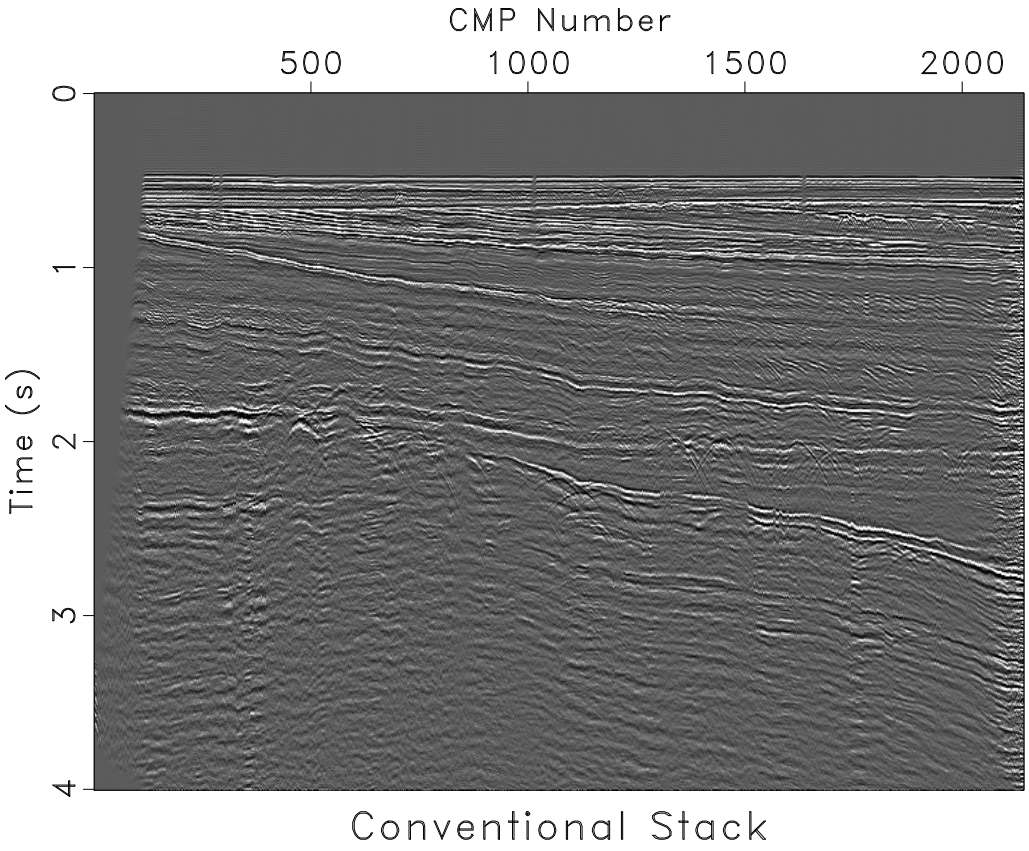

Figure 5.15: Viking Graben data example. NMO and stack using conventional method with 8-ms data as input. ch05-elf/viking nmostack

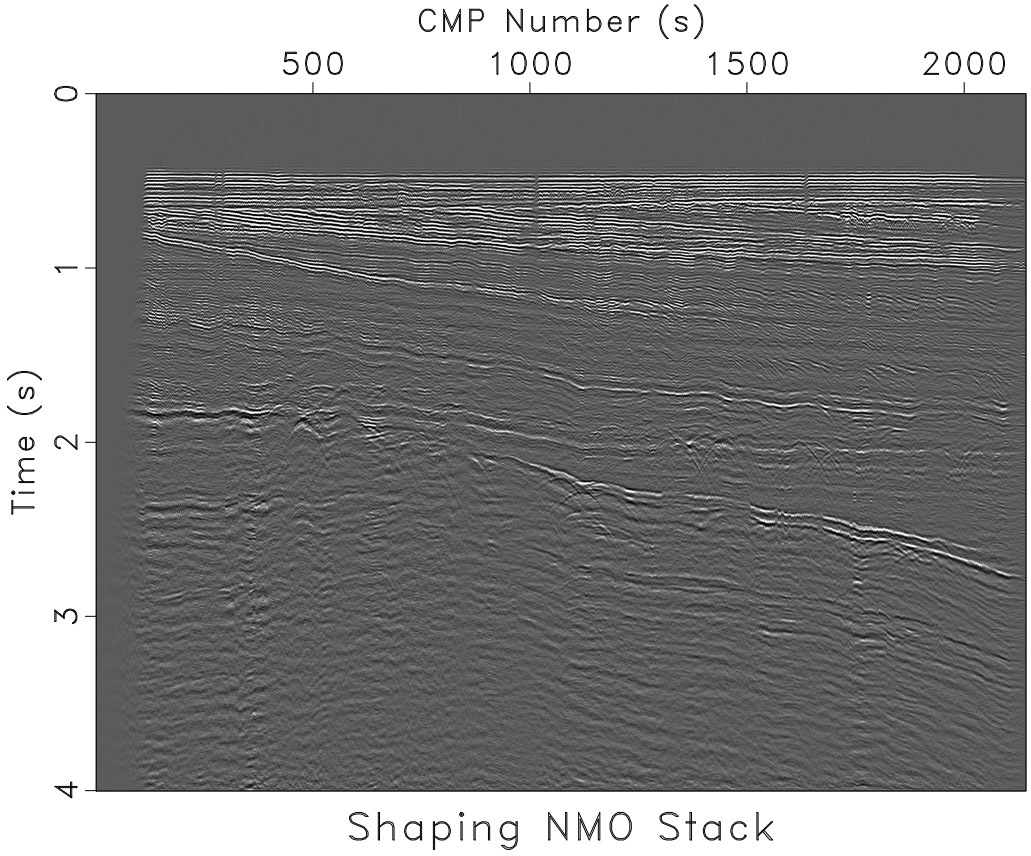

Figure 5.16: Viking Graben data example. NMO and stack using shaping NMO stack with 8-ms data as input. ch05-elf/viking shgmres1

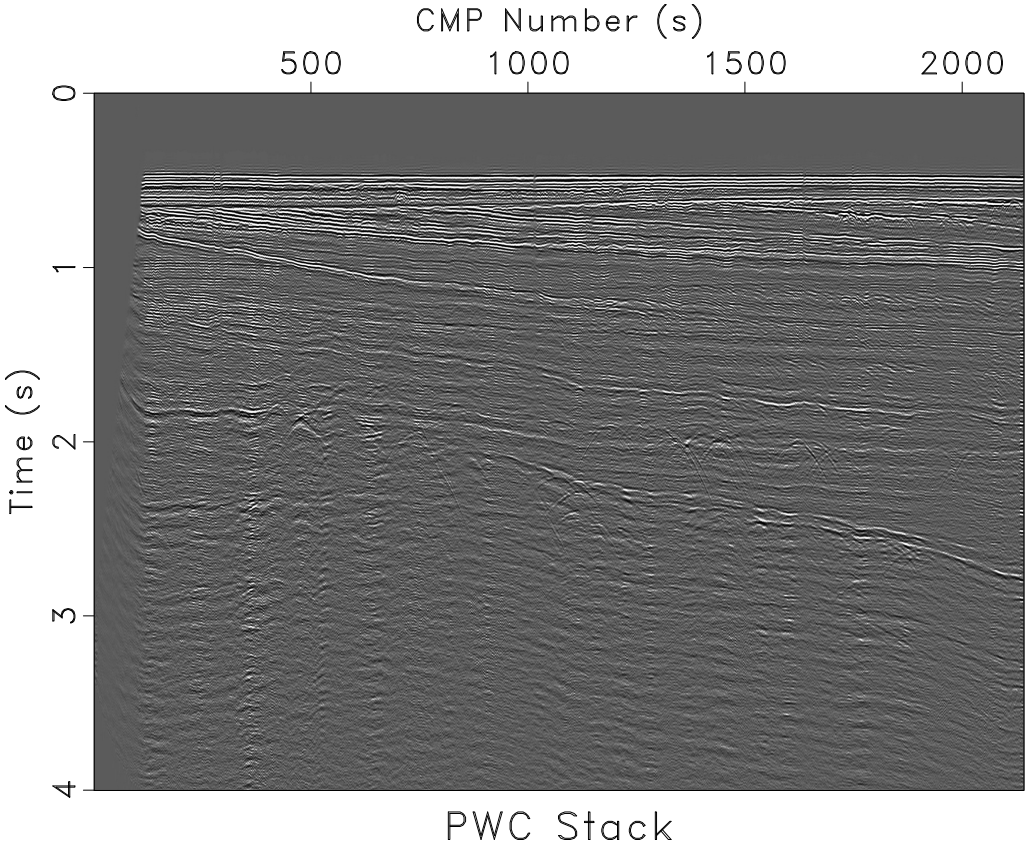

Figure 5.17: Viking Graben data example. NMO and stack using PWC stack with 8-ms data as input. ch05-elf/viking pwgmres

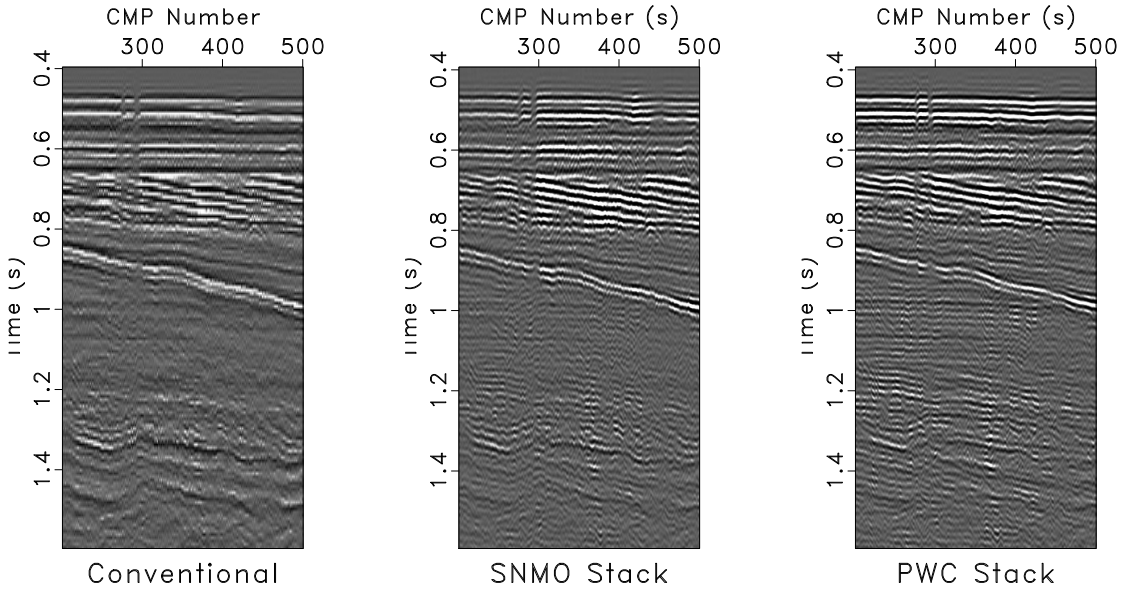

Figure 5.18: Zoomed in section of the Viking Graben data using (a) conventional NMO and stack (b) shaping NMO stack and (c) PWC stack. ch05-elf/viking cwstack,shwstack,pwwstack

Chapter 6

Conclusions

Conventional NMO stack can result in lower resolution stacked sections due to distortions caused by NMO correction and stretch muting. Treating the process of NMO and stack using regularized inversion allows us to compute an optimal stack with higher frequency content and denser temporal sampling. As indicated by numerical experiments with synthetic data, the recovered high frequency content is not limited by the sample rate of the input data and is consistent with the that of the reference trace for both shaping NMO and PWC stacking approaches. Furthermore, both stacking algorithms eliminate the effects of "NMO stretch", which contributes to the bandwidth of the reconstructed stack. Low frequency content also plays an important role in seismic data processing and imaging. As demonstrated by the synthetic and real data examples, PWC and shaping NMO stack both have the ability to recover lower frequencies compared to the conventional stack. The final stacked sections of the North Sea datasets have improved bandwidth and higher resolution, which may aid in interpretation and inversion of small-scale features such as thin layers and diffractions.

The main difference between the two approaches described in this thesis is that PWC stack follows local slopes of the data, while shaping NMO stack relies on velocity to compute the stack based on the conventional principles of NMO correction and stack. One benefit of shaping NMO stack, as demonstrated in the synthetic

and real data examples, is its ability to recover lower frequency content. Advantages of PWC stack include its relative insensitivity to non-hyperbolic moveout and AVO effects. Furthermore, PWC stack recovered higher frequencies in the real data examples and converged in fewer iterations in comparison with shaping NMO stack. In the examples presented, both algorithms effectively reduce the effects of "NMO stretch" and improve the bandwidth of the final stack.

By treating NMO and stack as an iterative inversion using shaping regularization, resolution is gained by utilizing signals from different offsets and minimizing stretching effects to reconstruct a high resolution stack that is not necessarily limited by the Nyquist frequency of the input data. In seismic processing, NMO and stack is a simple process applied to data. However, the same principles applied here can be extended to more complex processes, such as prestack migration, to achieve higher resolution results. With the increase in computational power, the extension of the inversion process that is proposed in this thesis to migration deserves further investigation and has the possibility to significantly enhance resolution in the resulting image.

Bibliography

Barnes, A. E., 1992, Another look at NMO stretch: Elsevier Science Publishing Co., Inc.

Byun, B. S., and E. S. Nelan, 1997, Method and system for correcting seismic traces for normal moveout stretch effects: U.S. Patent, **5**, 684–754.

Claerbout, J., 1992, Earth soundings analysis: Processing versus inversion: Blackwell Science.

———, 1996, A prospect for super resolution: Stanford Exploration Project (SEP) Report 93, 133–136.

Dunkin, J. W., and F. K. Levin, 1973, Effects of normal moveout on a seismic pulse: Geophysics, **38**, 635–642.

Fomel, S., 2002, Applications of plane-wave destruction filters: Geophysics, **67**, 1946–1960.

———, 2006, Towards the seislet transform: 76th Annual International Meeting: SEG, 2847–2850.

———, 2007, Shaping regularization in geophysical estimation problems: **72**, no. 2, R29–R36.

———, 2008, Nonlinear shaping regularization in geophysical inverse problems: 78th Annual International Meeting, SEG, Expanded Abstracts, 2046–2051.

———, 2010, Predictive painting of 3-D seismic volumes: Geophysics, **75**, no. 4, A25–A30.

Fomel, S., and A. Guitton, 2006, Regularizing seismic inverse problems by model

reparameterization using plane-wave construction: Geophysics, **71**, no. 5, A43–A47.

Fomel, S., and Y. Liu, 2010, Seislet transform and frame: Geophysics, **75**, no. 3, V25–V38.

Hicks, G. J., 2001, Removing nmo stretch using the Radon and Fourier- Radon transforms: 63rd Annual Conference and Exhibition, EAGE, Extended Abstracts, A–18.

Hilterman, F., and C. V. Schuyver, 2003, Seismic wide-angle processing to avoid nmo stretch: 73rd Annual International Meeting, SEG, Expanded Abstracts, 215–218.

Kazemi, N., and H. R. Siahkoohi, 2011, Local stretch zeroing NMO correction: **188**, no. 1, 123–130.

Keys, R. G., and D. J. Foster, 1998, Comparison of seismic inversion methods on a single real data set: Tulsa: Society of Exploration Geophysicists.

Kroode, F., S. Bergler, C. Corsten, J. W. de Maag, F. Strijbos, and H. Tijhof, 2013, Broadband seismic data - the importance of low frequencies: Geophysics, **78**, no. 2, WA3–WA14.

Liu, Y., S. Fomel, and C. Liu, 2015, Signal and noise separation in prestack seismic data using velocity-dependent seislet transform: Geophysics, **80**, no. 6, A25–A30.

Ma, Y., W. Zhu, Y. Luo, and P. Kelamis, 2015, Super-resolution stacking based on compressive sensing: SEG, 3502–3506.

Masoomzadeh, H., P. J. Barton, and S. C. Singh, 2010, Nonstretch moveout correction of long-offset multichannel seismic data for subbasalt imaging: Example from the north atlantic: Geophysics, **75**, no. 4, R83–R91.

Miller, R. D., 1992, Normal moveout stretch mute on shallow-reflection data: Geophysics, **57**, no. 11, 1502–1507.

Perroud, H., and M. Tygel, 2004, Nonstretch NMO: Geophysics, **69**, 599–607.

Rashed, M., 2014, Fifty years of stacking: Acta Geophysica, **62**, no. 3, 505–528.

Ronen, S., 1987, Wave-equation trace interpolation: Geophysics, **52**, no. 7, 973–984.

Ronen, S., and C. Liner, 2000, Least-sqaures DMO and migration: Geophysics, **65**, no. 5, 1364–1371.

Rupert, G. B., and J. H. Chun, 1975, The block move sum normal moveout correction: Geophysics, **40**, 17–24.

Saad, Y., and M. Schultz, 1986, GMRES: A generalized minimal residual algorithm for solving nonsymmetric linear systems: SIAM, **7**, no. 3, 856–869.

Shatilo, A., and F. Aminzadeh, 2000, Constant normal-moveout (CNMO) correction: a technique and test results: Geophysical Prospecting, **48**, 473–488.

Silva, M., M. Porsani, and B. Ursin, 2015, Recursive stack to zero offset along local slopes: SEG Technical Program Expanded Abstracts, 4323–4327.

Smith, G. C., and P. M. Gidlow, 1987, Weighted stacking for rock property estimation and detection of gas: Geophysical Prospecting, **35**, 993–1014.

Stark, T. J., 2013, Signal recovery beyond conventional Nyquist: The sample rates used for seismic acquisition do not need to limit the maximum recoverable frequencies: The Leading Edge, **32**, no. 11, 1334–1339.

Sun, Y., 1997, Inverse NMO stack in depth-variable velocity: Stanford Exploration Project (SEP) Report 94, 213–222.

Swan, H. W., 1988, Amplitude versus offset analysis in a finely layered media: SEG, 1195–1198.

Trickett, S., 2003, Stretch-free stacking: 73rd Annual International Meeting, SEG, Expanded Abstracts, 2008–2011.

Wisecup, R. D., 1998, Unambiguous signal recovery above the Nyquist using random-sample-interval imaging: **62**, no. 2, 763–771.

Yilmaz, O., 2001, Seismic data analysis: Processing, inversion, and interpretation of seismic data: SEG.

Zhang, B., K. Zhang, S. Guo, and K. Marfurt, 2013, Nonstretching nmo correction of prestack time-migrated gathers using a matching-pursuit algorithm: Geophysics, **78**, no. 1, U9–U18.

Zhdanov, M. S., 2002, Geophysical inverse theory and regularization problems: Geophysics, **57**, no. 5, 749–751.

Vita

Kelly Regimbal was born in Yorba Linda, California. After graduating from El Dorado high school in 2009, Kelly attended Colorado Mesa University in Grand Junction, Colorado to pursue a bachelor's degree in mathematics with minors in statistics and geology. After graduating in 2014, Kelly began her graduate studies in geophysics at the University of Texas at Austin. She started as a member of the Texas Consortium for Computational Seismology at the Bureau of Economic Geology.

Permanent address: 3796 Rose Drive, Yorba Linda, CA 92886

This thesis was typeset with LaTeX[†] by the author.

[†]LaTeX is a document preparation system developed by Leslie Lamport as a special version of Donald Knuth's TeX Program.